

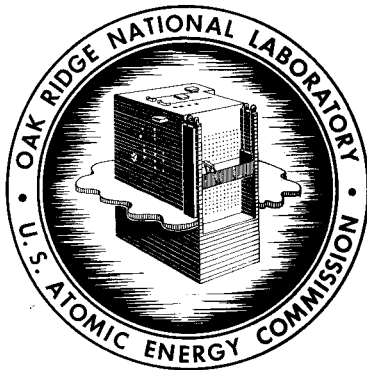


3 4456 0364202 0

ORNL-3028  
UC-25 - Metallurgy and Ceramics

FAST-FLUX MEASUREMENTS IN THE ORR CORE

P. Dragoumis  
J. R. Weir  
G. W. Leddicotte



**OAK RIDGE NATIONAL LABORATORY**

operated by

**UNION CARBIDE CORPORATION**

for the

**U.S. ATOMIC ENERGY COMMISSION**

Printed in USA. Price **\$1.25**. Available from the  
Office of Technical Services  
Department of Commerce  
Washington 25, D. C.

LEGAL NOTICE

This report was prepared as an account of Government sponsored work. Neither the United States, nor the Commission, nor any person acting on behalf of the Commission:

- A. Makes any warranty or representation, expressed or implied, with respect to the accuracy, completeness, or usefulness of the information contained in this report, or that the use of any information, apparatus, method, or process disclosed in this report may not infringe privately owned rights; or
- B. Assumes any liabilities with respect to the use of, or for damages resulting from the use of any information, apparatus, method, or process disclosed in this report.

As used in the above, "person acting on behalf of the Commission" includes any employee or contractor of the Commission, or employee of such contractor, to the extent that such employee or contractor of the Commission, or employee of such contractor prepares, disseminates, or provides access to, any information pursuant to his employment or contract with the Commission, or his employment with such contractor.

ORNL-3028

Contract No. W-7405-eng-26

METALLURGY DIVISION

FAST-FLUX MEASUREMENTS IN THE ORR CORE

P. Dragoumis  
J. R. Weir, Jr.  
G. W. Leddicotte

DATE ISSUED

JAN 16 1961

OAK RIDGE NATIONAL LABORATORY  
Oak Ridge, Tennessee  
Operated by  
UNION CARBIDE CORPORATION  
for the  
U. S. ATOMIC ENERGY COMMISSION

MARTIN MARIETTA ENERGY SYSTEMS LIBRARIES



3 4456 0364202 0



## FAST-FLUX MEASUREMENTS IN THE ORR CORE

P. Dragounis,<sup>1</sup> J. R. Weir, G. W. Leddicotte<sup>2</sup>

### ABSTRACT

The necessity for measuring the fast-neutron flux in beryllium irradiation studies has led to mapping of the fast flux in two positions of the ORR. The axial neutron flux distributions for thermal, 0.70 Mev and 2.9 Mev, were measured using Co<sup>59</sup>, Np<sup>237</sup>, and S<sup>32</sup>, respectively. The methods used in the manufacture of the flux monitors and the techniques used in making the measurements are described in detail.

Axial-flux peaking in the ORR core occurs at about 3 in. below the reactor midplane. In the B-2 core position the thermal-flux peak is  $9.5 \times 10^{13}$  neutrons/cm<sup>2</sup>·sec when the reactor is at 20 Mw. The maximum fast-flux values in B-2 are  $8 \times 10^{13}$  neutrons/cm<sup>2</sup>·sec (greater than 0.7 Mev) and  $1.8 \times 10^{13}$  neutrons/cm<sup>2</sup>·sec (greater than 2.9 Mev). In the B-8 position maximum flux values were not measured. Observed fluxes were  $1.4 \times 10^{14}$  neutrons/cm<sup>2</sup>·sec (greater than 0.7 Mev) and  $2 \times 10^{13}$  neutrons/cm<sup>2</sup>·sec (greater than 2.9 Mev).

### INTRODUCTION

In recent years there has been increasing interest in the effects of fast-neutron irradiation on the physical and mechanical properties of materials. With the construction of new materials-testing reactors such as the Oak Ridge Research Reactor (ORR), increasing numbers of high-flux facilities are now available for experimentation.

When experimenting to observe the effects of fast-neutron bombardment of materials, it is necessary to know the magnitude and the spectral distribution of flux in the fast range. In studies of the effects of gas atoms produced by metal transmutations, viz, the Be<sup>9</sup> (n,2n) and Be<sup>9</sup> (n, $\alpha$ ) reactions in beryllium, it is necessary to measure the neutron-flux magnitudes in the energy ranges above

<sup>1</sup>American Electric Power Service Corporation, New York, New York.

<sup>2</sup>Analytical Chemistry Division

the thresholds for these reactions. The beryllium neutron reactions are described in Table I. Thus, it is necessary to choose flux-monitoring materials that exhibit properties consistent with the demands of the experiment and which are compatible with use in the reactor.

Current interest in the irradiation effects on beryllium caused by the gas-producing  $\text{Be}^9 (n,2n)$  and  $\text{Be}^9 (n,\alpha)$  reactions has led to an in-pile experimental program which is under way at present. It is the purpose of this report to present the methods and materials used for monitoring the neutron flux during two of the early beryllium irradiation experiments. Graphical presentation of data obtained in two ORR core positions is included herein.

#### DESCRIPTION OF THE ORR

The ORR is a light-water cooled and moderated Materials Testing Reactor-type research reactor fueled with enriched uranium in the form of boxed elements filled with curved fuel plates. These plates consist of an uranium-aluminum alloy clad with aluminum. A sketch of the ORR, a view of a typical fuel element, and a drawing of the core lattice are presented in Figs. 1, 2, 2a, and 3, respectively. A full technical description of the ORR can be found elsewhere.<sup>3</sup>

Experiments in the ORR core must be housed in a can, which is shaped and dimensioned exactly as are the fuel element boxes. The experiments occupy fuel element positions in the reactor and so must closely resemble the elements to avoid perturbation of the core-cooling water-flow distribution. Instrument and power leads that emanate from the experiment must be housed in a rigid vertical tube that has been designed as an integral part of the experiment facility. This requirement ensures that fuel elements and experiments occupying adjacent positions can be freely removed without interference.

In the period of interest to this presentation, the ORR operated at 20 Mw, on a four-week cycle, including a one-week shutdown. Midcycle refueling was often required and usually necessitated a shutdown of several hours.

---

<sup>3</sup>J. A. Cox and T. E. Cole, "Design and Operation of the ORR," Proceedings of the Second U.N. Conference on the Peaceful Uses of Atomic Energy 10(Research Reactors), 86 (1958).

TABLE I. Fast-Neutron Reactions in Beryllium\*

Reaction	Energy Threshold (Mev)	Effective Threshold (Mev)	Cross Section (barns)
<u>(n,2n)</u>			
$\text{Be}^9 + n \rightarrow \text{Be}^8 + 2n$	2.7	2.7	0.600
$\text{Be}^8 \rightarrow 2 \text{He}^4$			
<u>(n,<math>\alpha</math>)</u>			
$\text{Be}^9 + n \rightarrow \text{He}^4 + \text{He}^6$	0.71	2.41	0.080
$\text{He}^6 \xrightarrow{\beta^-} \text{Li}^6$			
$\text{Li}^6 + n \rightarrow \text{He}^4 + \text{H}^3$	← Thermal →		945

\* C. E. Ells and E. C. W. Perryman, "Effects of Neutron-Induced Gas Formation in Beryllium," J. Nuclear Metals 1(1), 73 (April, 1959).

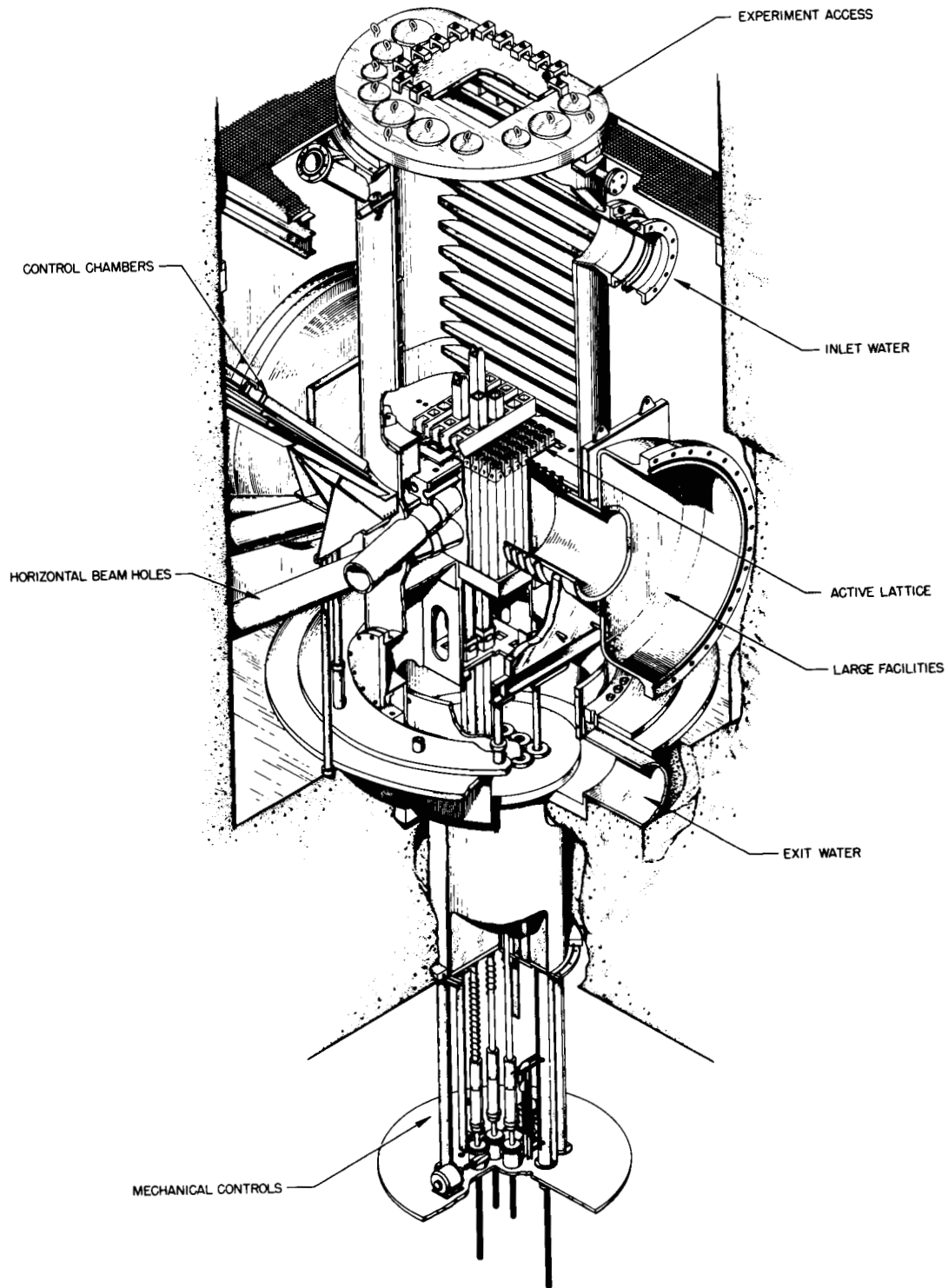


Fig. 1 View of the ORR Core and Tank.

UNCLASSIFIED  
PHOTO 41728

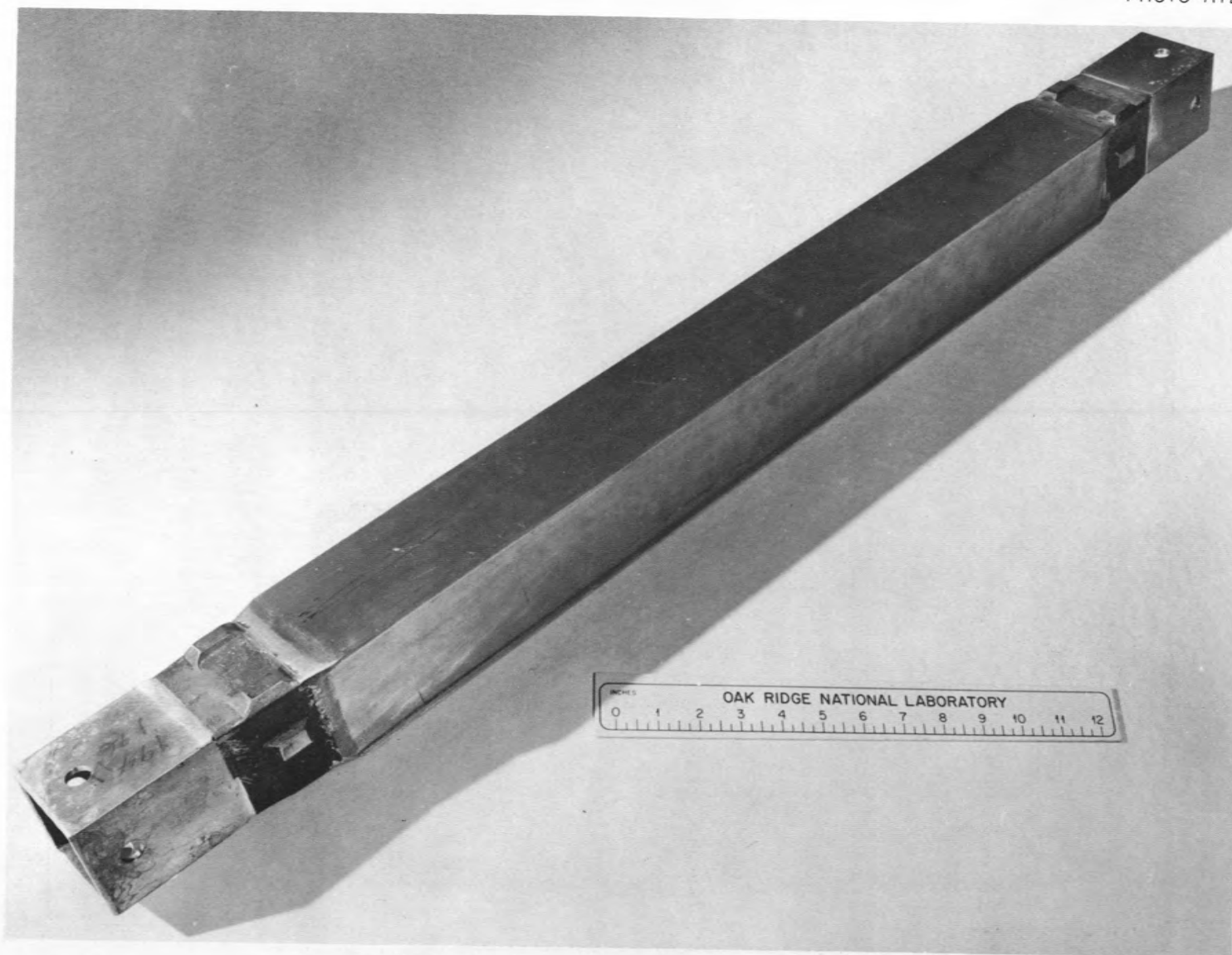


Fig. 2 A Typical ORR Fuel Element.

UNCLASSIFIED  
PHOTO 41730

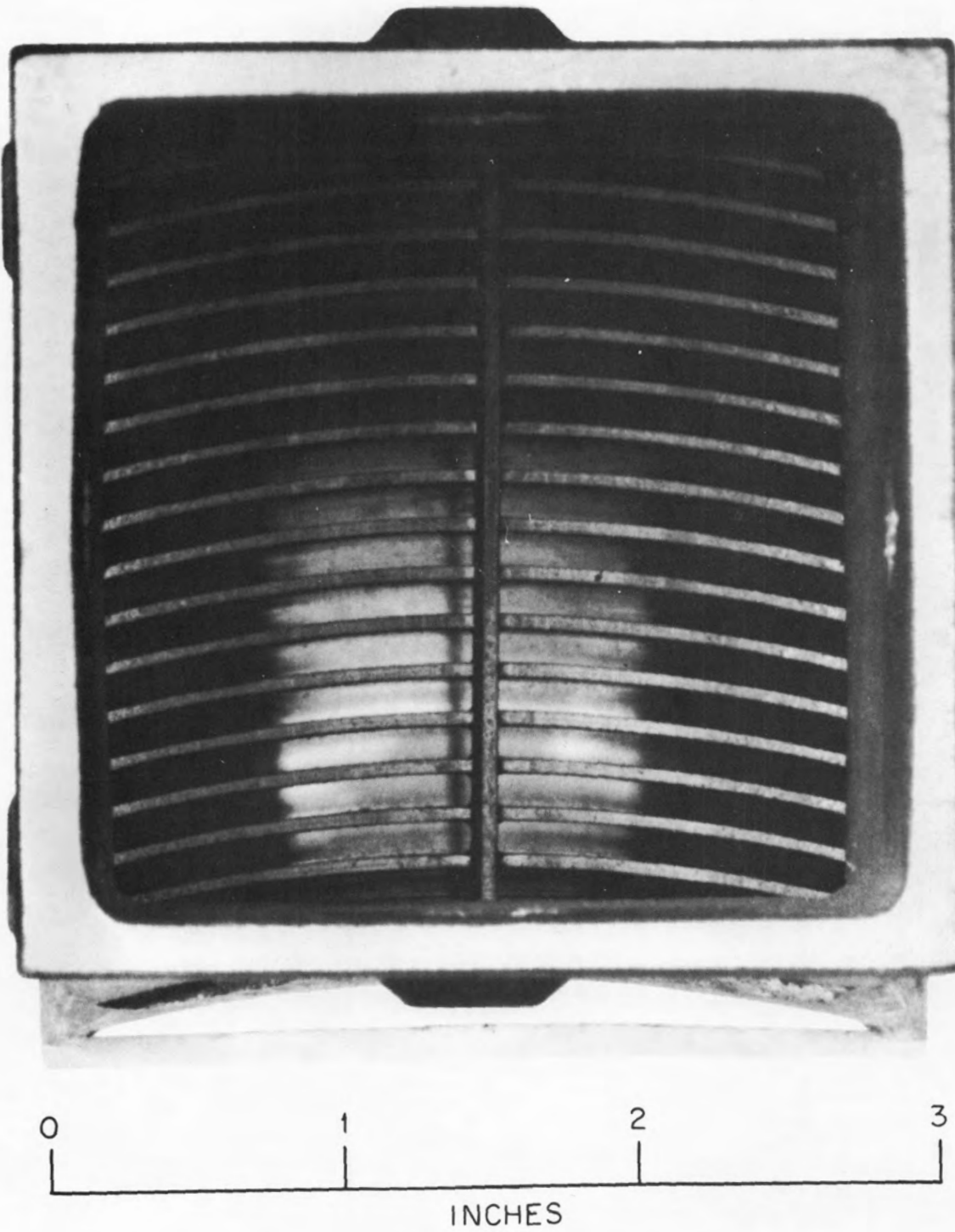


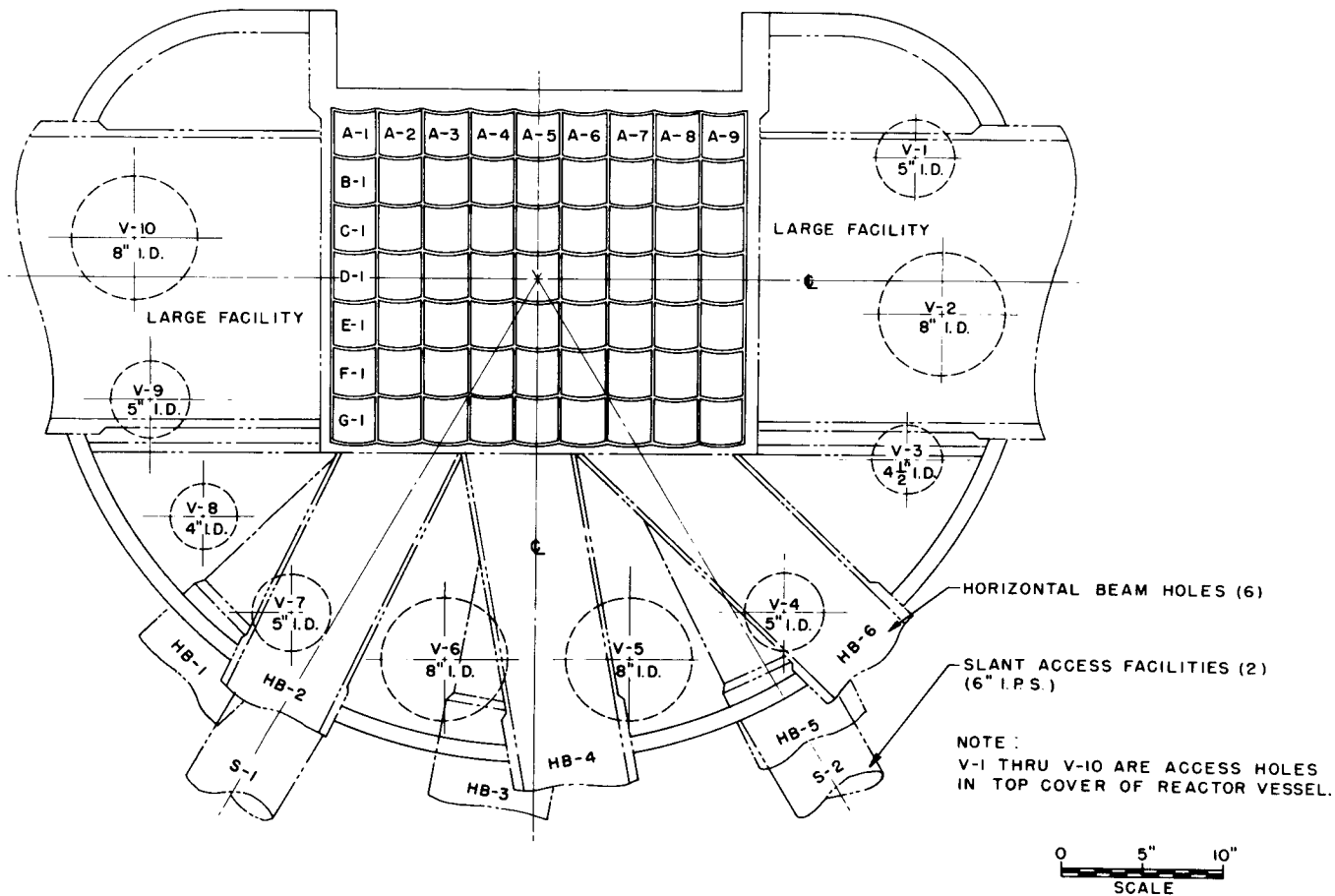
Fig. 2A End View of an ORR Fuel Element.

POOL FACILITY

UNCLASSIFIED  
DWG C33561

- KEY
-  EXPERIMENT
  -  FUEL
  -  BERYLLIUM
  -  SHIM ROD

LEGEND



-7-

Fig. 3 ORNL Research Reactor Lattice Pattern and Experiment Locations.

## SELECTION OF MONITORING MATERIALS

In order to investigate the effects of neutron-induced helium on the dimensional stability and mechanical properties of beryllium, several in-pile experiments have been conducted at the Oak Ridge National Laboratory. In these experiments the two measured variables were temperature and neutron flux.

The neutron flux can be measured in several different ways.<sup>4</sup> However, when access to the reactor core is limited, the most convenient and simplest method is foil, powder, or wire activation.<sup>5</sup> In the activation method, the neutrons produced by the reactor interact with material of known cross sections and the flux is determined by a measurement of the induced radioactivities. These radioactivity measurements may be made either by nondestructive means (direct counting of the irradiated material) or following a destructive, or radiochemical separation of the desired radionuclides. The "activation" materials, or monitors, can be used to measure thermal, resonance (or epithermal), and fast-neutron flux and spectra in a reactor irradiation facility. Characteristics of some of the fast-neutron activation monitors, generally referred to as threshold detectors, are given in Table II and elsewhere.<sup>6,7,8</sup>

The  $\text{Be}^9(n,2n)$  and  $\text{Be}^9(n,\alpha)$  reactions, which have energy thresholds<sup>9</sup> of 2.7 and 0.70 Mev, respectively, are the significant mechanisms by which helium is produced in beryllium. Consequently, any observations of property changes in irradiated beryllium must, in order to be understood, be accompanied by an accurate knowledge of neutron flux in the energy range of interest. Ideally, monitoring

<sup>4</sup>J. W. Baum, Neutron Dosimetry - A Review, UR-381 (1955).

<sup>5</sup>P. M. Uthe, Jr., Attainment of Neutron-Flux Spectra From Foil Activations, USAFIT-TR-57-3 (1957).

<sup>6</sup>L. E. Steele and J. R. Hawthorne, Neutron Flux Measurements for Materials Irradiation Experiments at ANL, BNL, ORNL, and NRTS, NRL-5483 (May, 1960).

<sup>7</sup>W. J. Price, Nuclear Radiation Detection, pp. 270, 283-85, 292-93, McGraw-Hill, New York, 1958.

<sup>8</sup>J. B. Trice, "Measuring Reactor Spectra with Thresholds and Resonances," Nucleonics 16(7), 81-83 (July, 1958).

<sup>9</sup>The energy threshold is that level of energy at which the reaction begins to occur.

TABLE II. Properties of Some Fast-Flux Monitors

Material	Reaction	Half-Life	Effective Threshold (MeV) <sup>a,b</sup>	Reaction Cross Section (barns)
Np <sup>237</sup>	Fission	Dependent on which	0.70	1.9 <sup>c</sup>
U <sup>238</sup>	Fission	fission product is	1.45	0.54 <sup>c</sup>
Th <sup>232</sup>	Fission	selected for counting	1.75	--
P <sup>31</sup>	(n,p) Si <sup>31</sup>	2.6 hr	2.5	--
S <sup>32</sup>	(n,p) P <sup>32</sup>	14.3 days	2.9	0.370
Ni <sup>58</sup>	(n,p) Co <sup>58</sup>	72 days	5.0	0.084 <sup>d</sup>
Al <sup>27</sup>	(n,p) Mg <sup>27</sup>	9.8 min	5.3	--
Si <sup>28</sup>	(n,p) Al <sup>28</sup>	2.3 min	6.1	--
Mg <sup>24</sup>	(n,p) Na <sup>24</sup>	15.0 hr	6.3	--
Al <sup>27</sup>	(n, $\alpha$ ) Na <sup>24</sup>	15.0 hr	8.6	--

<sup>a</sup>L. E. Steele and J. R. Hawthorne, Neutron Flux Measurements for Materials Irradiation Experiments at ANL, BNL, ORNL and NRTS, NRL-5483 (May, 1960).

<sup>b</sup>W. J. Price, Nuclear Radiation Detection, pp. 270, 283-85, 292-93, McGraw-Hill, New York, 1958.

<sup>c</sup>D. J. Hughes and R. B. Schwartz, Neutron Cross Sections, BNL-325, 2nd ed., (July, 1958).

<sup>d</sup>C. E. Mellish, "Threshold" Reaction Cross-Sections in Reactors - An Inter-comparison, AERE-R-3251 (1960).

Note: Data published by C. E. Mellish confirmed by G. W. Leddicotte and W. J. Hampton, ORNL Analytical Chemistry Division (to be published).

materials having thresholds similar to those of the two beryllium-neutron reactions would be suitable, especially if the energy dependence of both the monitor and the beryllium-reaction cross sections were similar in the range of interest. The energy dependence of the monitoring-reaction cross section is the only requirement dictated directly by the nuclear properties of the observed metal, beryllium.

The primary considerations for choosing the monitoring materials include the fabricability of the material into usable form, the half-life of the radioactive product to be measured, the interference produced by competing reactions, and the energy of the radiations emitted by that product. Moreover, the physical arrangement of the reactor and experimental facility, the order of magnitude of the neutron flux to be measured, and the temperature of the medium in which the monitor is to be placed, all impose further restrictions on the choice of a suitable material.

Table II lists several fast monitors which were readily available at ORNL. Neptunium-237 with an effective threshold<sup>10</sup> of 0.70 Mev,  $P^{31}$  with an effective threshold of 2.5 Mev, and  $S^{32}$  with an effective threshold of 2.9 Mev can be singled out as having desirable thresholds with respect to the  $Be^9 (n,2n)$  and  $Be^9 (n,\alpha)$  reactions. The  $S^{32} (n,p)$  reaction has been successfully used by several experimenters.<sup>11,12</sup> The end product  $P^{32}$ , decays with a 14.3 day half-life, which is compatible with a one-month irradiation and subsequent two-to-three week delay before remote disassembly facilities can be procured and the monitors delivered for analysis and counting. The  $P^{31} (n,p) Si^{31}$  reaction will saturate too quickly because of the 2.6 day half-life of the product  $Si^{31}$  and would probably decay to a low level before

---

<sup>10</sup>If the energy dependent cross section curve were replaced by an idealized curve having a step increase in cross section at some energy  $E_t$  from zero to a constant cross section, that value  $E_t$  is the effective threshold.

<sup>11</sup>L. E. Steele and J. R. Hawthorne, Neutron Flux Measurements for Materials Irradiation Experiments at ANL, BNL, ORNL and NRTS, NRL-5483 (May, 1960).

<sup>12</sup>J. C. Zukas and R. G. Berggren, "Flux Measurements and Irradiation Assemblies Used in the LITR, MTR and ORR Reactors," Proceedings AEC Welding Forum (Oct., 1959).

counting could be accomplished. Sulfur-32, therefore, is the only listed detector that is practical for the beryllium application, having an effective threshold of 2.9 Mev compared with 2.7 Mev for the  $\text{Be}^9 (n,2n)$  and 2.41 Mev for the  $\text{Be}^9 (n,\alpha)$  reaction.

Neptunium-237 has an effective threshold identical to the energy threshold of the  $\text{Be}^9 (n,\alpha)$  reaction (0.70 Mev), but it should be noted that the effective threshold of the  $\text{Be}^9 (n,\alpha)$  reaction, as stated in Table I is 2.41 Mev. Therefore, the neptunium monitors serve mostly to provide information about the flux above 0.70 Mev which is useful in determining the spectral distribution of neutrons. Neptunium-237 undergoes a fission reaction and provides several products, the radioactivity of which may be counted and measured for flux determination.

The energy-dependent cross sections of the  $\text{Np}^{237}$  fission and  $\text{S}^{32} (n,p)$  monitoring reactions are compared with those of the  $\text{Be}^9 (n,2n)$  and  $\text{Be}^9 (n,\alpha)$  helium-producing reactions in Figs. 4 and 5.

The two beryllium reactions described previously were not considered for use in determining flux because analysis for the gaseous reaction products,  $\text{He}^4$  and  $\text{H}^3$  is difficult.<sup>13</sup> Moreover, since the measurement of  $\text{He}^4$  gas content is accomplished by a destructive process, it would have to await completion of mechanical tests and metallographic inspection. This would have delayed computation of flux, which was needed for other experiments.

The activation cross section should also be considered in choosing a monitoring material. In low-intensity reactors it is possible that unreasonable exposure times may be required to accumulate sufficient radioactivity for accurate counting if monitors having low activation cross sections are used. The ORR has a flux of approx  $1 \times 10^{14}$  neutrons/cm<sup>2</sup>·sec (greater than 0.70 Mev as measured with  $\text{Np}^{237}$ ) in the two experimental positions under discussion and so allows the use of monitoring reactions having low cross sections.

Sulfur and neptunium were selected as primary monitoring materials for the beryllium experiment. Monitors containing  $\text{Co}^{59}$  were included to measure the thermal flux, which was needed for computation of  $\text{He}^4$  generated by the lithium-thermal

<sup>13</sup>C. E. Ells and E. C. W. Perryman, "Effects of Neutron-Induced Gas Formation in Beryllium," J. Nuclear Metals 1(1), 73 (April, 1959).

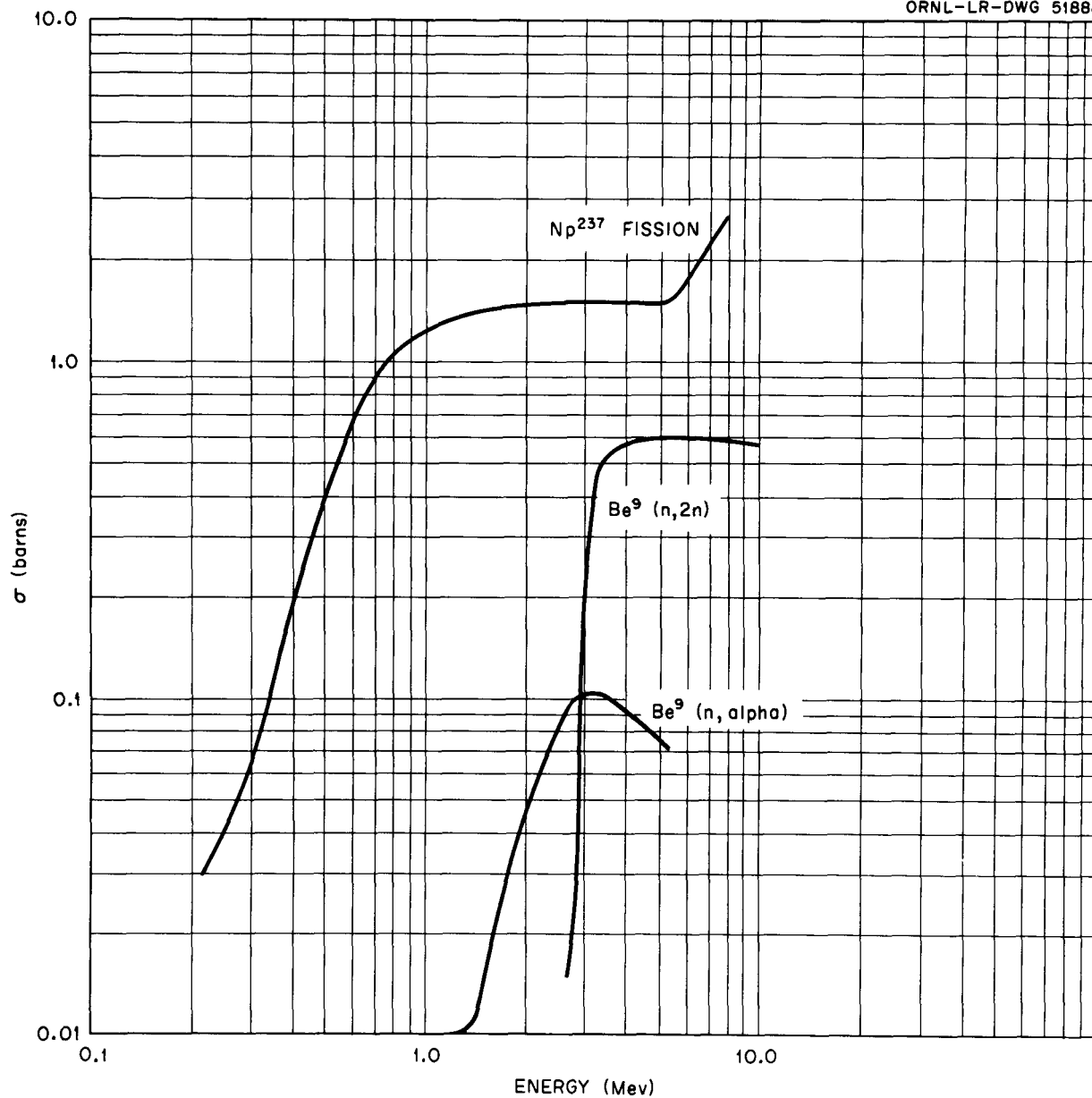


Fig. 4 Cross Sections for the  $\text{Np}^{237}$  Fission,  $\text{Be}^9 (n,2n)$  and  $\text{Be}^9 (n,\alpha)$  Reactions. REF: D. J. Hughes and R. B. Schwartz, Neutron Cross Sections BNL-325, 2nd ed. (July, 1958).

UNCLASSIFIED  
ORNL-LR-DWG 51889

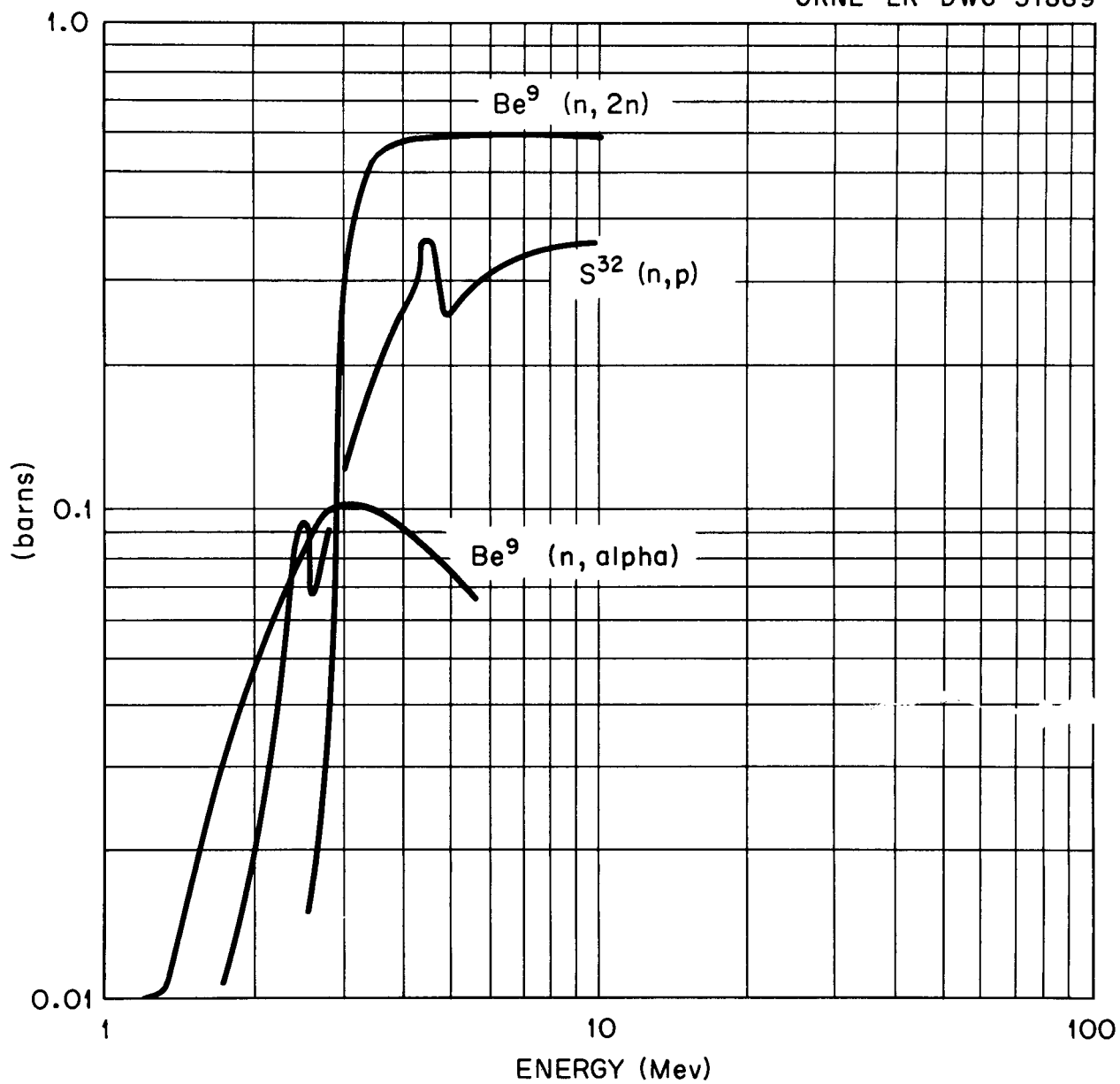


Fig. 5 Cross Sections for the  $S^{32} (n,p)$ ,  $Be^9 (n,2n)$  and  $Be^9 (n,\alpha)$  Reactions. REF: D. J. Hughes and R. B. Schwartz, Neutron Cross Sections BNL-325, 2nd ed. (July, 1958).

neutron reaction described in Table I. The  $\text{Co}^{59}$  undergoes an  $(n,\gamma)$  reaction producing  $\text{Co}^{60}$  (5.27 y). Uranium-238 monitors were added to supplement fast measurements and to provide further spectral breakdown.

#### DESCRIPTION OF THE FLUX MONITORING FACILITY

The flux monitoring facility shown in Fig. 6 was incorporated into the beryllium-experiment can as shown in Fig. 7. The "Y"-shaped monitor holder penetrates the can in three places. At the top, the two points emerge and serve as holes for the insertion of the tubes containing the monitors. These top holes also serve as entrance orifices for the influent core-cooling water. The stem of the "Y" penetrates the bottom of the experiment can and serves as an exit for the cooling water. The core pressure differential drives the water through this "Y" holder, thereby cooling the monitors. The right-angle bends in the holder serve as natural stops for the inserted monitor tubes.

As is shown in Figs. 6 and 8, the monitor tube consists of a 1/4-in. stainless steel tube, of thin wall, filled with monitors and equipped with a handle which protrudes from the top of the experiment can. This handle enables the reactor operators to remove or insert the monitor tube during shutdowns without disturbing the experiment facility. Each tube is marked with the position that it is to occupy (e.g., southwest corner, B-8 core position).

In determining the effect of the experimental section of the irradiation facility on the flux attenuation between the two monitor holes, it may be assumed that the exposure can was filled with aluminum, the volume of the Be samples being neglected.

The position of each individual monitor with respect to the ORR centerline is obtained indirectly. When the monitor tube is to be filled with some ten to twelve monitors, the position of each sample is measured with respect to the bottom of the monitor tube and, since this tube always rests at the right-angle bend in the "Y" holder, this point is used as a reference. The distance between this reference and the reactor centerline is a known constant, so the actual position of each monitor with respect to the reactor centerline can be arithmetically determined.

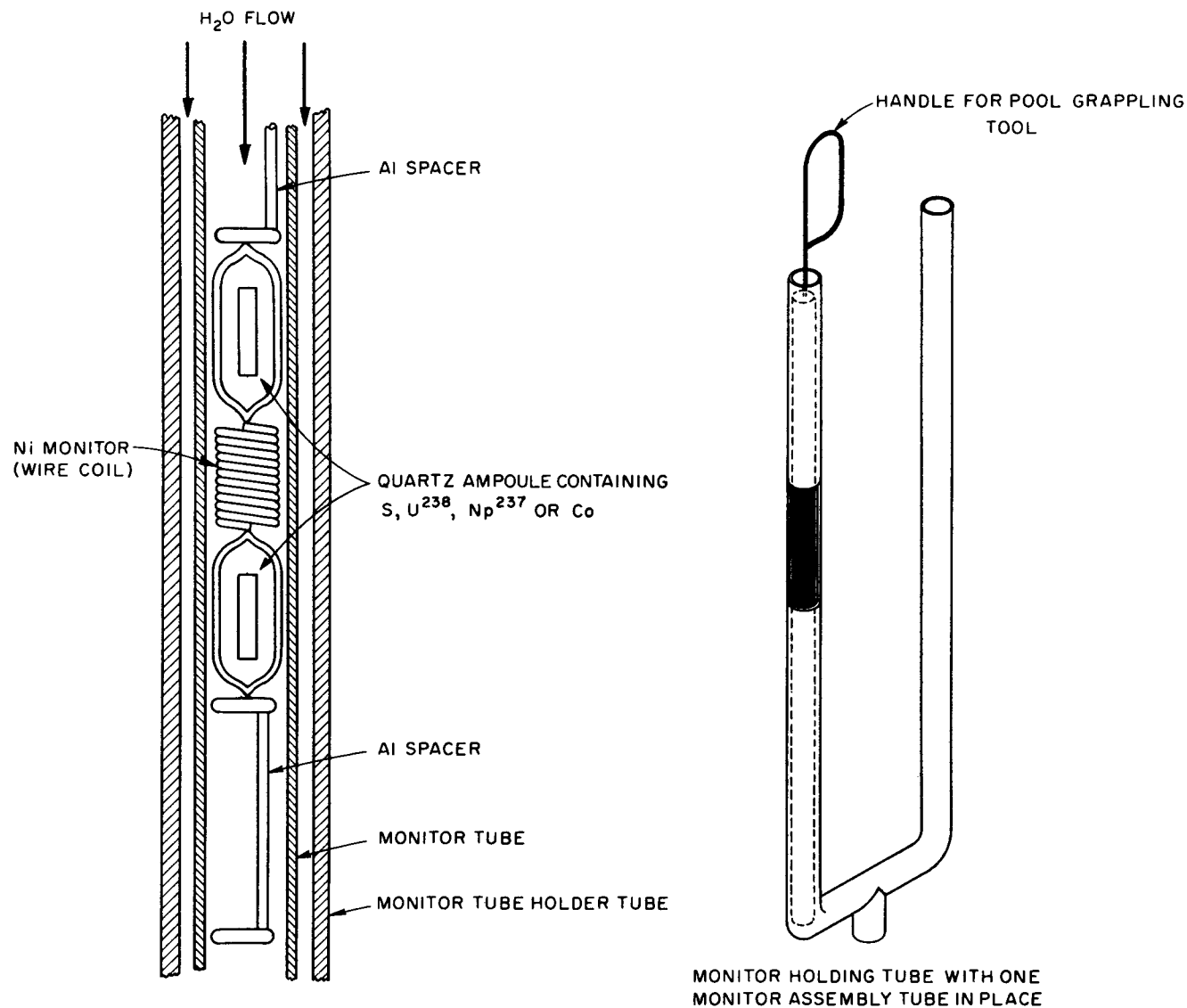


Fig. 6 Flux Monitoring Facility.

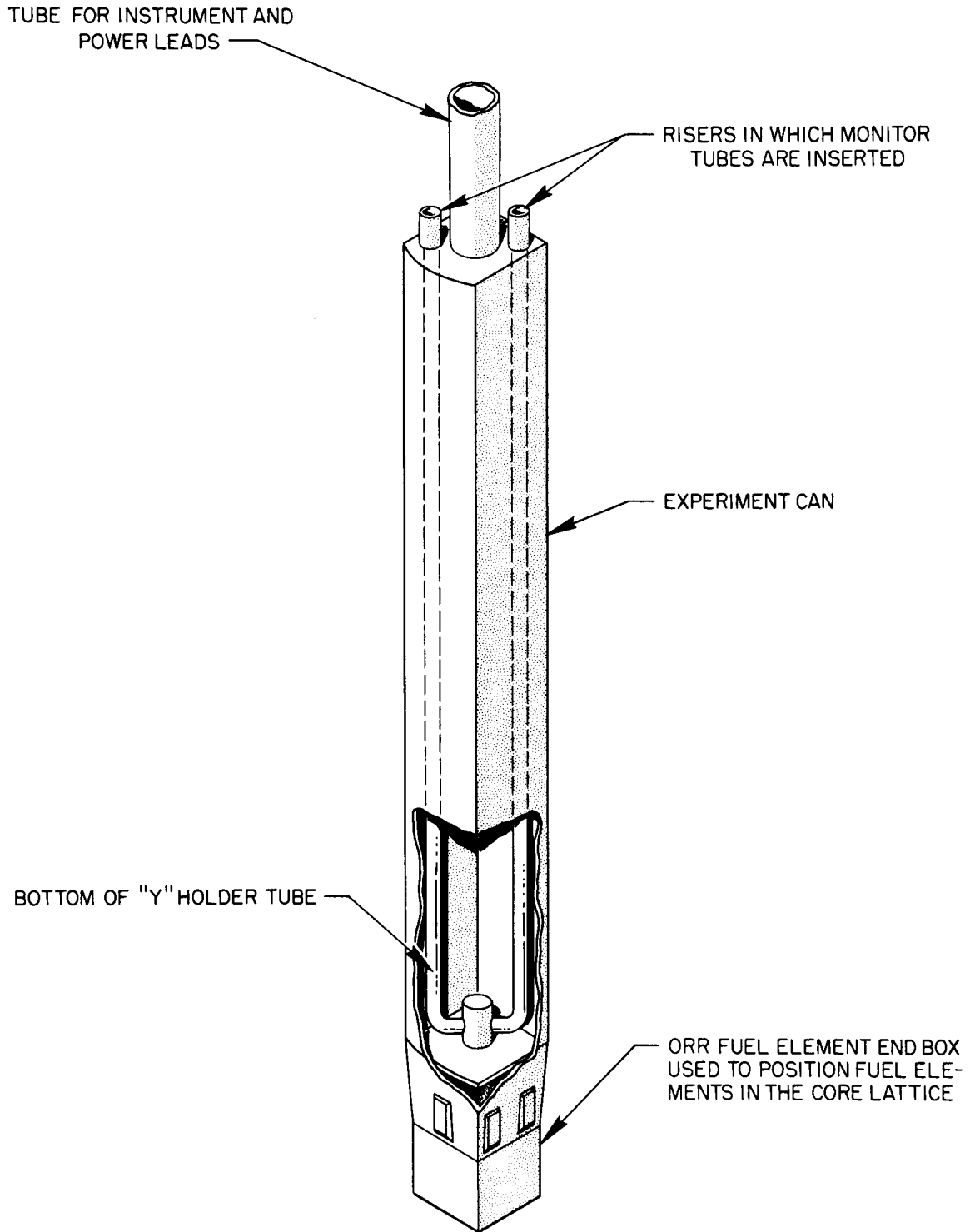


Fig. 7 "Y" Monitor Holder Tube Shown Installed in Experiment Can.

Unclassified  
Y-36397

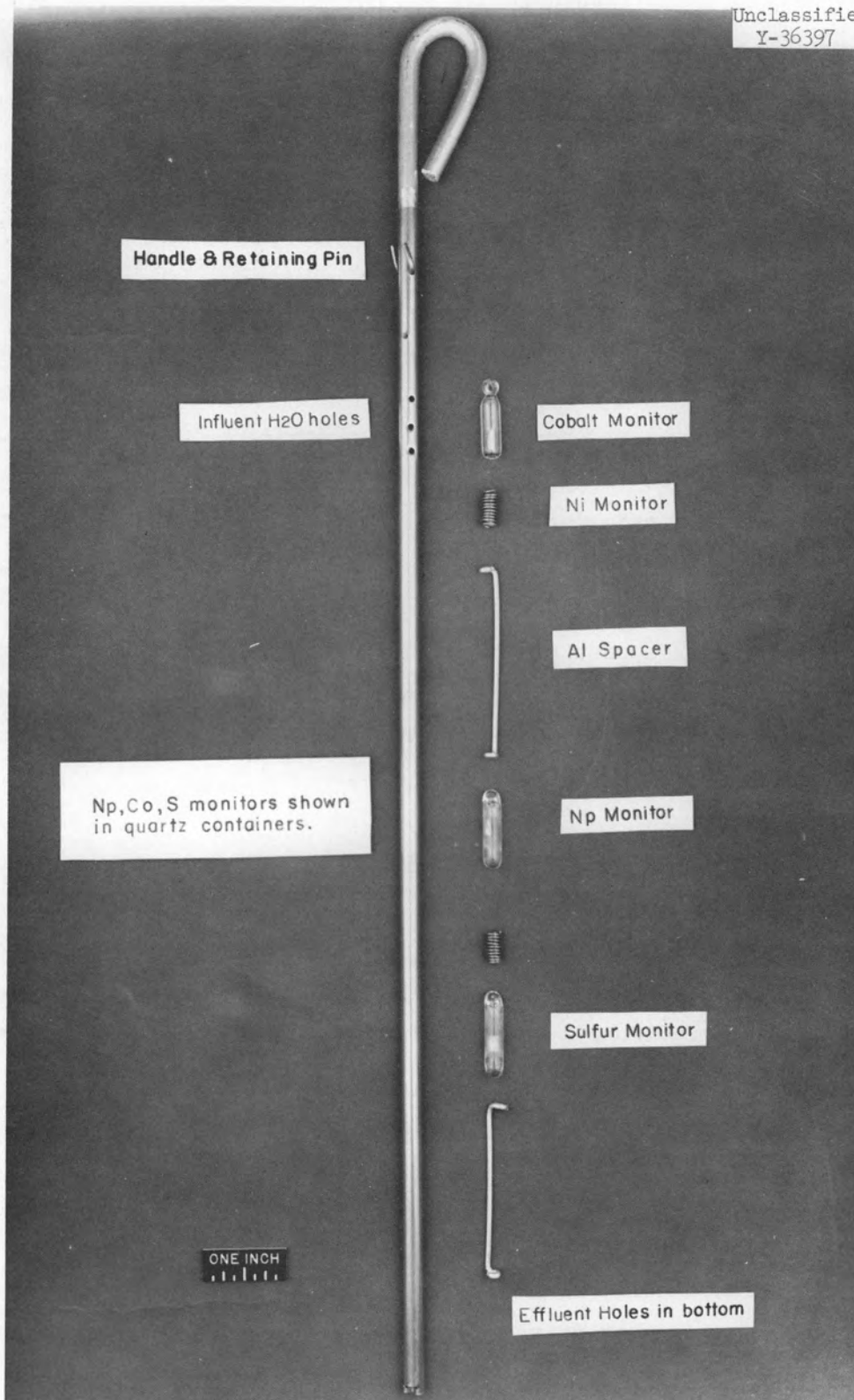


Fig. 8 Monitor Assembly Tube and Components.

The monitor tubes are disassembled in hot cells and each ampoule placed in a separate container and identified before delivery to the assayer.

#### FABRICATION OF INDIVIDUAL MONITORS

The neptunium and uranium monitor material is vapor deposited on a 0.010-in. x 1/2-in. square aluminum foil. The coated foil is then folded and inserted into the quartz ampoule which is 1 in. long x 3/16 in. in diameter. The amount of these materials deposited per foil is about 0.10 mg. Sulfur monitors are made by compacting sulfur powder into pellets which are then encapsulated in similar quartz ampoules. Pieces of cobalt-aluminum alloy (in foil or wire form) are directly encapsulated and used for thermal-neutron monitoring purposes. Nickel, which is just being tried in present experiments, is made into monitors simply by coiling high-purity wire. No container is used with the nickel monitors.

Uranium-aluminum wire is now being used in place of the vapor-deposited uranium monitors and also is used encapsulated. Encapsulation of the monitors in quartz ampoules is intended to minimize loss or radioactive contamination of the material during irradiation and handling. In all instances the monitors are contained in the rig in the manner previously described.

#### PROCESSING OF IRRADIATED MONITORS

As has been previously pointed out, the induced radioactivity in a monitor can be measured either by nondestructive or destructive techniques. The decay characteristics of each radionuclide subsequently used to obtain a measurement of the different neutron-energy components of the flux spectrum are given in Table III.

Each of these radionuclides is sufficiently long enough in half-life so that a considerable amount of time can be allowed for dismantling the experimental rig after the irradiation in order to ensure reasonable radiation safety practices. Also, shorter lived radionuclides induced in the monitor materials (such as the aluminum alloys) and components of the experimental rig will have decayed away so

TABLE III. Radiation Characteristics of the Neutron-Induced Radionuclides Used in the Measurement of Flux<sup>a</sup>

Neutron Reaction	Induced Radionuclide Measured	Half-Life	Method of Decay	Radiation Energy (Mev)	
				Particles	Gamma
Np <sup>237</sup> (n,f) or	Ba <sup>140</sup>	12.8 days	$\beta^-$ , $\gamma$	1.022, 0.480	0.0296, 0.132, 0.162, 0.304, <u>0.537</u>
U <sup>238</sup> (n,f)	La <sup>140</sup> <sup>(b)</sup>	40 hr	$\beta^-$ , $\gamma$	1.32, 1.67 2.26	0.093, 0.3286 0.4867, 0.8151, <u>1.596</u>
S <sup>32</sup> (n,p)	P <sup>32</sup>	14.3 days	$\beta^-$	<u>1.70</u>	None
Ni <sup>58</sup> (n,p)	Co <sup>58</sup>	72 days	EC, $\beta^+$ , $\gamma$	0.47	<u>0.81</u> <sup>(c)</sup>
Co <sup>59</sup> (n, $\gamma$ )	Co <sup>60</sup>	5.27 years	$\beta^-$ , $\gamma$	0.306	1.3316, 1.1715, <u>2.50</u> (sum)

<sup>a</sup>From information given in "Table of Isotopes," by D. Stromenger, J. M. Hollander, and G. T. Seaborg, Reviews of Modern Physics 30(2), 585-904 (1958).

<sup>b</sup>As the daughter nuclide of Ba<sup>140</sup>; the 1.596 Mev gamma is used in radioactivity measurements.

<sup>c</sup>Also accompanied by the annihilation gamma radiations (0.51 Mev) formed by the decay of the  $\beta^+$  particles.

that minimum interferences in the handling and processing of the materials will be experienced. Likewise, the radiation energies are strong enough so that self-absorption within the monitor material during its processing is minimal.

With regard to the measurement of radioactivity, these radionuclides could have been measured either by beta or gamma counting methods. Price<sup>14</sup> gives a general description and indicates the type of instruments that can be used in radiation detection. In this work, it was found to be more practical to use gamma radioactivity methods employing gamma spectrometers. Crouthamel<sup>15</sup> presents the principles of gamma scintillation spectrometry and has given many examples of its application. He has also established criteria for considering such parameters as radiation intensity, efficiency of detection, geometry, etc.

A gamma spectrometer using a 3-in. x 3-in. NaI crystal and a 200-channel analyzer (manufactured by Radiation Instrument Detection Laboratories, Chicago, Illinois) has been employed to make the radioactivity measurements. In each monitor analysis by a nondestructive method, the irradiated monitor is mounted on a suitable backing (card, plastic, metal, glass, etc.) and placed on the crystal of the spectrometer. Counting times sufficiently long to collect enough counts for a statistical evaluation (e.g., 10 000 counts/min will give an accuracy and precision of  $\pm 1\%$ ) of the measurements were used. Standard samples of radioisotopes of known absolute radioactivity rate (as disintegrations per time unit) were counted under similar conditions in order to obtain the absolute disintegration rate of the irradiated monitor specimen.

In Table III, the underscored radiations were used to determine the radioactivity measurements on each specimen. It should be noted that in the measurement of the 1.70 Mev beta radiations from 14.3 day P<sup>32</sup> the bremsstrahlung (the emission of secondary electromagnetic radiation produced by deceleration of charged particles passing through matter) resulting from the absorption of these particles by the materials composing the housing of the crystal detector is conveniently measured by counting the sample specimen in a simple, or gross, gamma counter (manufactured by Atomic Instrument Company, Cambridge, Massachusetts). Standard samples of P<sup>32</sup>

<sup>14</sup>W. J. Price, Nuclear Radiation Detection, pp. 270, 283-85, 292-93, McGraw-Hill, New York, 1958.

<sup>15</sup>C. E. Crouthamel, Applied Gamma-Ray Spectrometry, Pergamon Press, 1960.

were assayed in the same manner as a basis for the analysis of each sulfur monitor. The absolute disintegration rate of each standard radioisotope has been determined in the manner described by Reynolds.<sup>16</sup>

In some instances it has been desirable to radiochemically process the uranium-aluminum and neptunium-aluminum monitors in order to separate the Ba<sup>140</sup> from other radioactive components in the monitor. These components originate either as contaminants in the aluminum or as shorter lived fission-product radionuclides. The method of radiochemical analysis following the dissolution of the monitor in a suitable acid mixture (5HCl:1HNO<sub>3</sub>) is that given by Leddicotte.<sup>17</sup> Either the 0.537 Mev gamma of the freshly separated Ba<sup>140</sup> or the 1.596 Mev gamma of La<sup>140</sup> after it has come into equilibrium with Ba<sup>140</sup> is measured by gamma scintillation spectrometry.

In each radioactivity measurement, the purity of separation, or freedom from contaminant radioactivity can be checked. Standard practices involving decay measurements and additional gamma spectrometry techniques are followed in order to assure maximum reliability of results.

#### CALCULATION OF FLUX DATA

The flux data presented elsewhere in this report were computed from radioactivity measurements by use of the following general equation:

$$\phi = \frac{A}{D\sigma_{ac} SK} \quad (1)$$

where  $\phi$  = the flux or number of neutrons bombarding the target nuclei in the sample, neutrons/cm<sup>2</sup>.sec.

A = the experimentally determined amount of radioactivity, disintegrations per second.

---

<sup>16</sup>S. A. Reynolds, Assay Methods Used in the ORNL Radioisotope Program, ORNL-CF 60-2-39 (Feb., 1960).

<sup>17</sup>G. W. Leddicotte, "Neutron Activation Analysis for Barium," Method No. 5 11080, Oak Ridge National Laboratory Master Analytical Manual, TID-7015, Section 5 (May, 1960).

D = the number of target nuclei in the monitor.

$\sigma_{ac}$  = the activation cross section for the neutron reaction,  $\text{cm}^2/\text{target nucleus}$ .

S = a factor established for the production of radioactivity, A, in a given period of irradiation in a reactor.

K = a factor established as a correction factor for the decay of the desired radioelement from the termination of the experiment to the time of radioactivity measurement.

The radioactivity, A, is corrected for any dilution factor, chemical yield if a radiochemical separation is made, etc. The number of atoms, D, is calculated on the basis that the element nuclei are in normal isotopic ratio (except for  $\text{U}^{238}$ , which is an enriched isotope). The number of atoms entering into the neutron reaction can be calculated as follows:

$$D = \frac{(\text{weight of monitor})(\text{concentration of element nuclei})(\text{Avogadro's number})}{\text{Molecular Weight of Nuclei}} \quad (2)$$

The activation cross section values used are those tabulated in Table II.

The factor established, S, for the production of the radioactivity to be measured is considered to be a saturation factor,  $1 - e^{-\lambda t}$ , or the ratio of the amount of radioactivity produced in an irradiation time  $t$  to the amount produced in an infinite time of irradiation. Here,  $\lambda$  is the decay constant for the radioelement of interest ( $\lambda = 0.693/\text{radioelement half-life}$ ).

The decay correction factor, K, is based on the relation  $e^{-\lambda t}$  where  $t$  is the elapsed time from the termination of the reactor experiment to the time of radioactivity assay;  $\lambda$  is again the decay constant for the radioelement of interest. Variations in reactor power level, short shutdown periods, etc., are considered in calculating S and K.

#### RESULTS OF FLUX MEASUREMENTS

The two core positions (B-2 and B-8) in which the flux data were obtained are shown in Fig. 9. Also shown is the core configuration which existed during the reported cycles. Results were obtained in the northeast and southwest corners of



those two positions. In Fig. 9 it can be seen that when the experiment was occupying the B-2 position (for which it was originally designed), the northeast corner was closest to the radial center of the core and the southwest corner was in a minimum flux location for that position. In the B-8 position, however, both the southwest and northeast corners were almost equidistant from the radial center of the core, with the southwest corner receiving more flux. Also evident from the configuration shown in Fig. 9 is that the B-8 position should receive the greater flux magnitude, while the B-2 position lacking a fuel element in the adjacent C-2 position should receive lower flux. The flux data corroborate these observations.

In a test reactor, such as the ORR, several experiments are operated simultaneously and some of these are wired to scram the reactor when experimental malfunctions occur. These unscheduled shutdowns often necessitate refueling (because of xenon buildup) before the reactor can be restarted. Moreover, the removal and insertion of various pieces of experimental equipment can bring about changes in the core fuel loading from cycle to cycle. These changing conditions can affect both the flux magnitude and the radial and axial distribution.

If flux data are to be obtained over a number of reactor cycles, either by multicycle or many single-cycle measurements, core loadings, configuration, and shim rod positions must be known in order to correlate and interpret the data. Knowledge of these details can also facilitate estimation of the neutron flux in adjacent core positions. The irradiation history of the flux-monitoring runs are summarized in Table IV and the ORR core loadings and shim rod positions for the cycles in which measurements were made are presented in Figs. 10 through 15A. The flux data for the B-2 and B-8 positions as measured with Co, Np, and S are presented in Figs. 16 through 21. Uranium-238 data are not available because the monitors that were used contained too much  $U^{235}$  and the resultant thermal fission overshadowed the fast fission results.

Figures 16 through 18 represent the data obtained in ORR core position B-2. It should be noted that Figs. 16 and 18 include curves taken during two succeeding ORR cycles (Table IV) and that the flux magnitude and axial distribution are observed to be coincident even though the Series II data are very limited in number.

The spread between the curves obtained in the northeast and southwest corners of the B-2 position was different in the cobalt, neptunium, and sulfur measurements

TABLE IV. Irradiation History of Monitoring Runs<sup>a,b</sup>

Monitor Series	Corresponding ORR Cycle No.	Duration of Exposure (days)	Approx Average Power Level (Mw)	Comments
I	20	22.6	20	Single-cycle Irradiation
II	21	23	20	Single-cycle Irradiation
IV	24 and 25	40.8	16	Two-cycle Irradiation of monitors

<sup>a</sup>J. A. Cox, Reactor Operations and Radioactive Wastes Operations Quarterly Report January-March 1960, ORNL-CF 60-3-148, pp. 5-7 (May, 1960).

<sup>b</sup>J. A. Cox, Reactor Operations and Radioactive Wastes Operations Quarterly Report April-June 1960, ORNL-CF 60-6-127, pp. 5-7 (Aug., 1960).

Note: Series III monitors were damaged during removal and are excluded from consideration in this presentation.

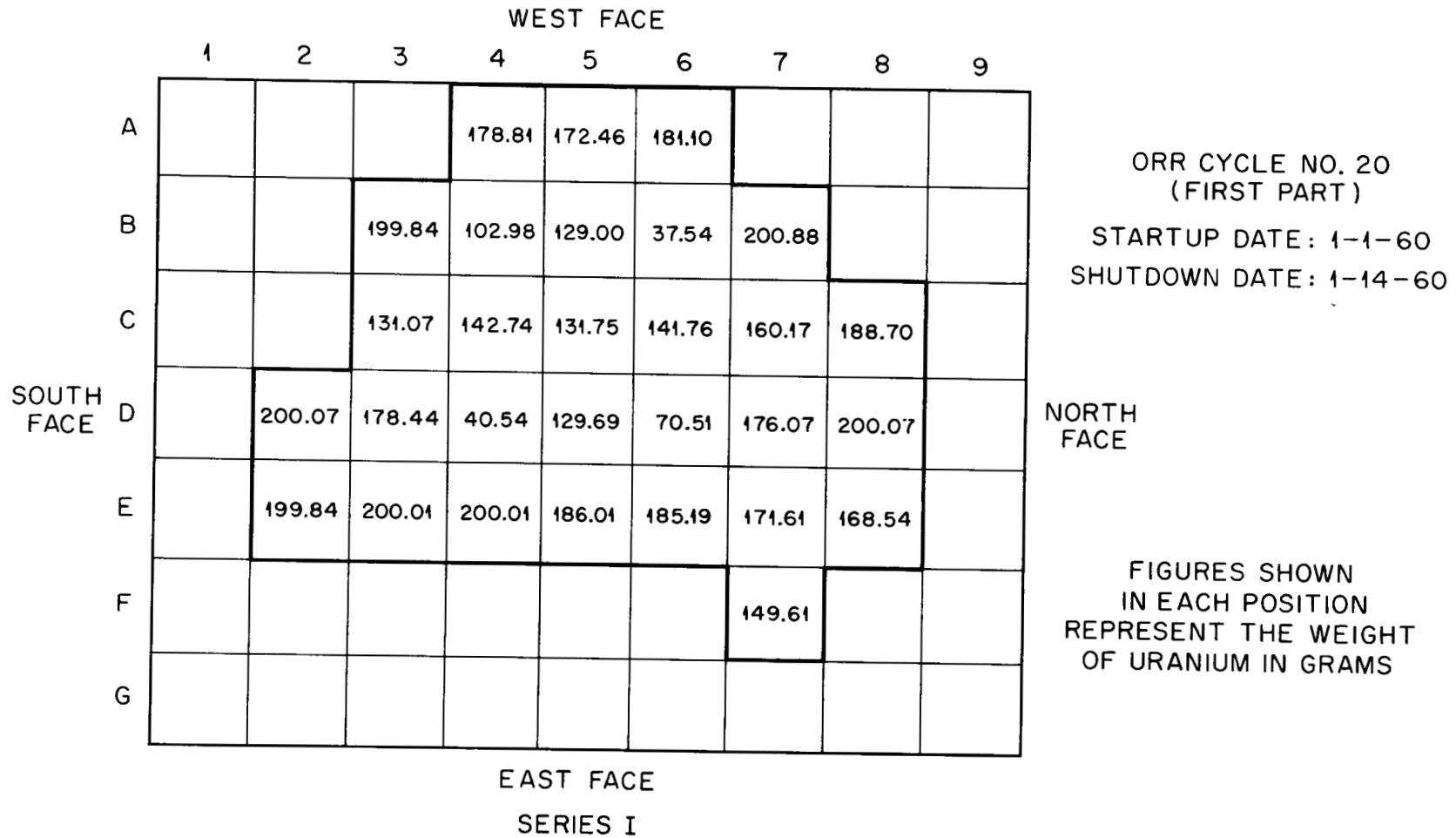


Fig. 10 ORR Cycle 20; ORR Core Configuration.

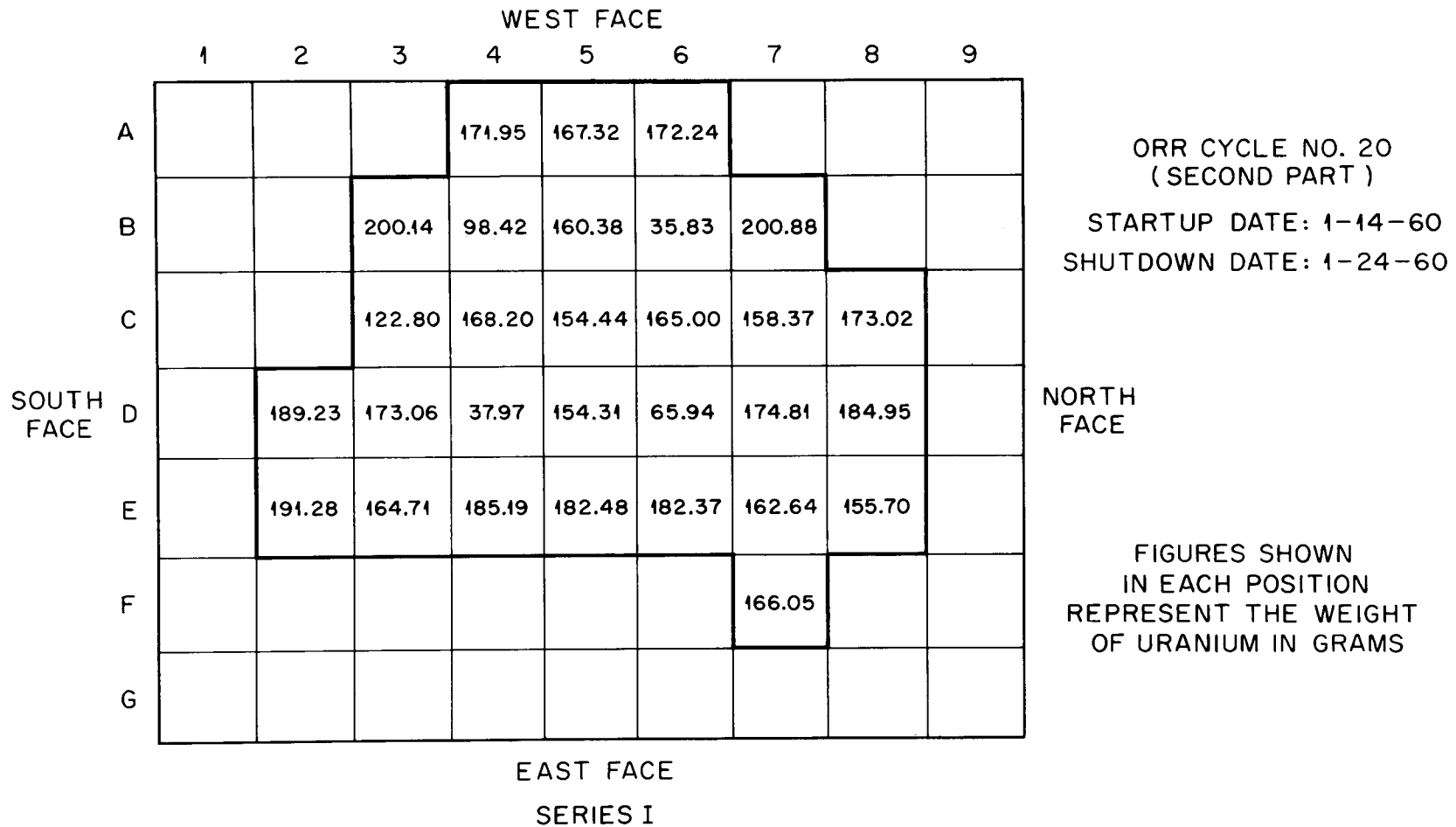


Fig. 10A ORR Cycle 20; ORR Core Configuration.

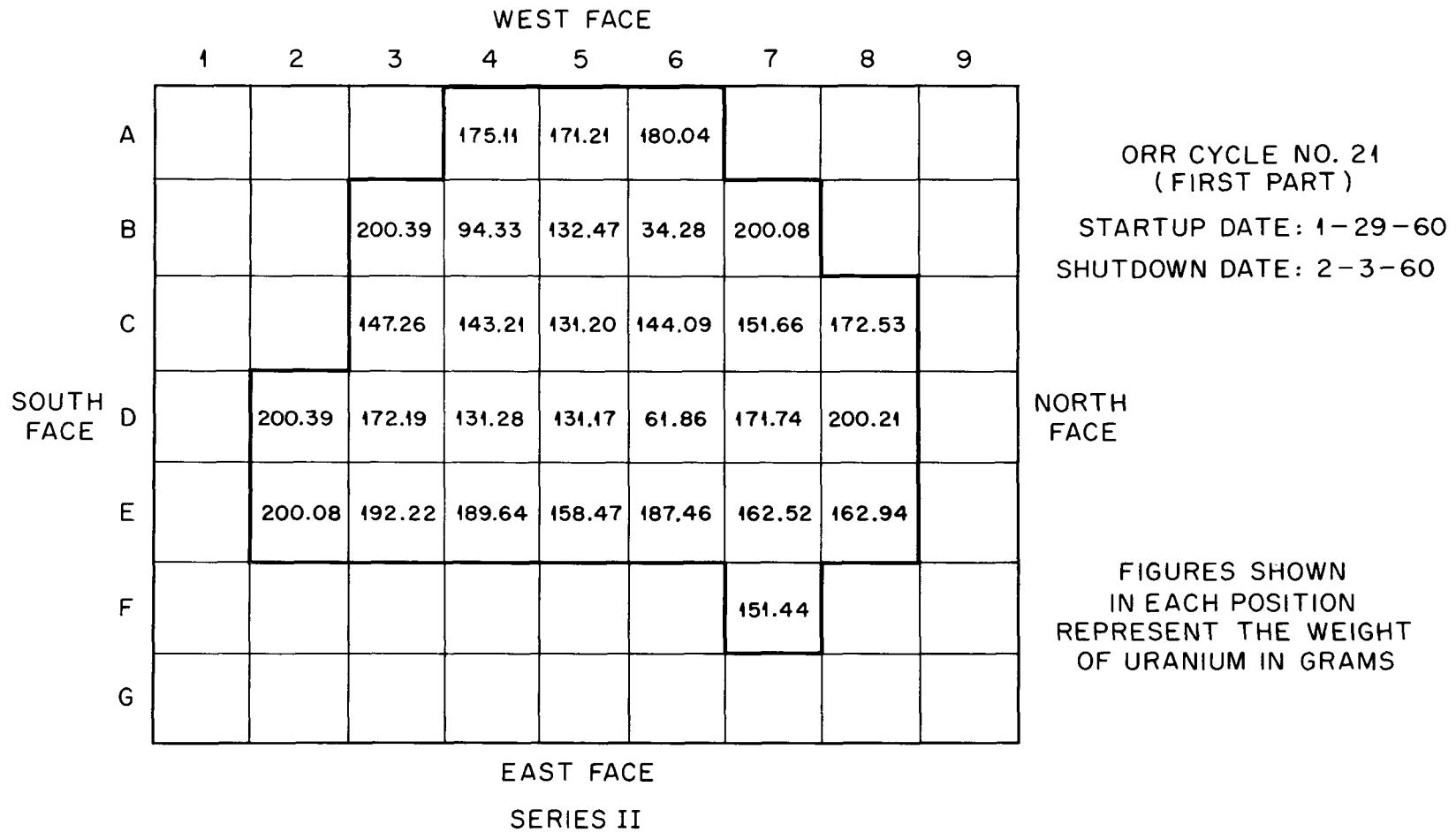


Fig. 11 ORR Cycle 21; ORR Core Configuration.

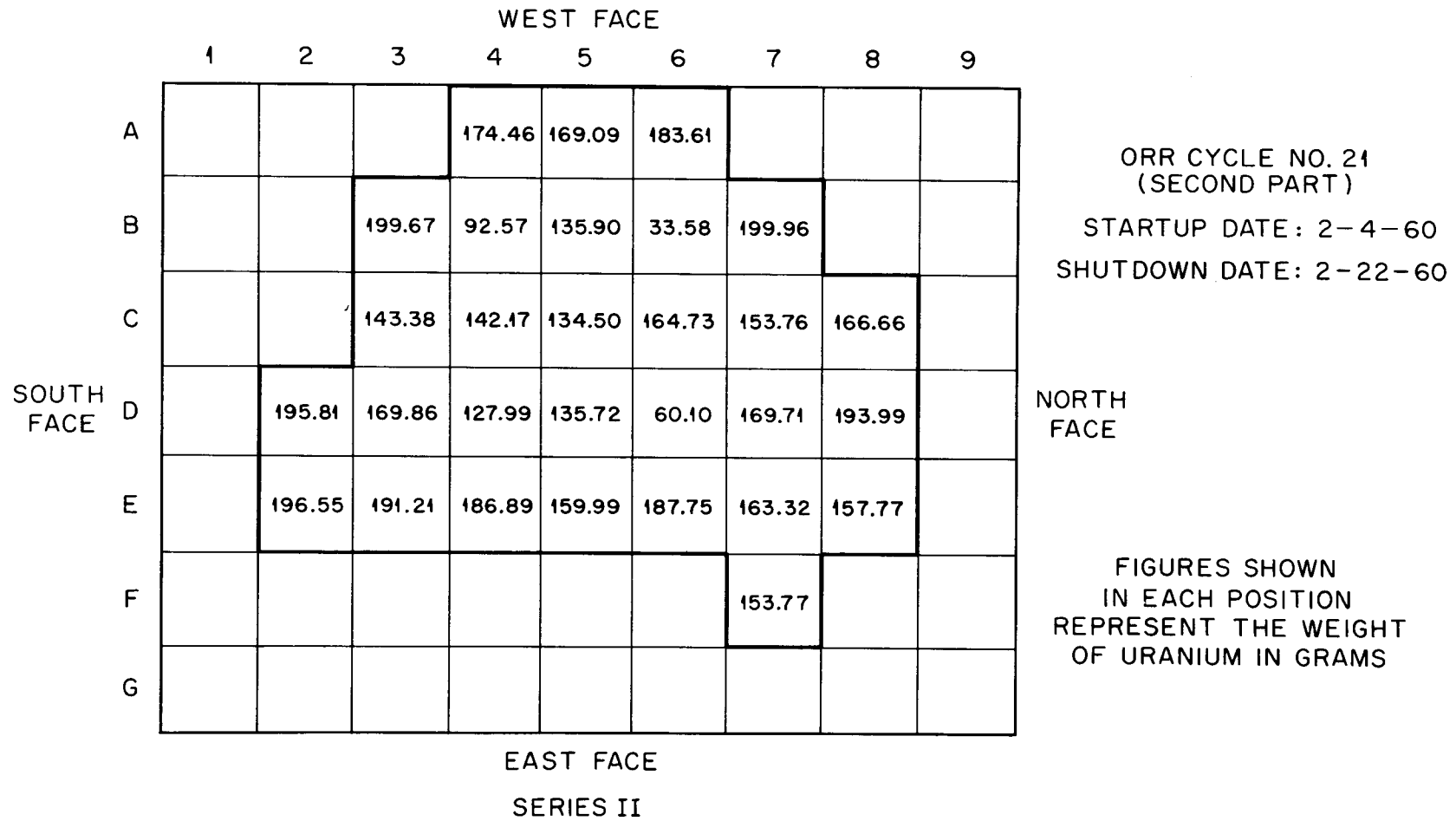


Fig. 11A ORR Cycle 21; ORR Core Configuration.

		WEST FACE								
		1	2	3	4	5	6	7	8	9
SOUTH FACE	A				162.68	169.49	166.34			
	B			192.76	42.28	153.54	109.84	189.12		
	C			131.05	147.78	163.36	179.87	187.82	161.25	
	D		159.07	189.12	91.05	161.09	69.22	187.72	141.96	
	E		159.83	189.23	188.48	185.37	185.94	187.21	161.74	
	F							148.54		
	G									
		EAST FACE								
		SERIES IV*								

ORR CYCLE NO. 24  
(ENTIRE CYCLE)  
STARTUP DATE: 4-22-60  
SHUTDOWN DATE: 5-14-60

FIGURES SHOWN  
IN EACH POSITION  
REPRESENT THE WEIGHT  
OF URANIUM IN GRAMS

NORTH  
FACE

\*SERIES IV MONITORS  
WERE IRRADIATED  
OVER TWO ORR CYCLES  
(NOS. 24 AND 25)

Fig. 12 ORR Cycle 24; ORR Core Configuration.

		WEST FACE								
		1	2	3	4	5	6	7	8	9
SOUTH FACE	A				168.82	169.64	167.39			
	B			191.69	131.64	135.40	101.09	188.36		
	C			147.70	147.29	163.48	179.88	199.94	144.08	
	D		145.67	199.94	81.85	142.95	60.47	157.03	144.18	
	E		146.73	199.94	200.07	177.88	175.07	199.98	145.70	
	F							148.00		
	G									
		EAST FACE SERIES IV*								

ORR CYCLE NO. 25  
(FIRST PART)

STARTUP DATE: 5-21-60  
SHUTDOWN DATE: 5-22-60

FIGURES SHOWN  
IN EACH POSITION  
REPRESENT THE WEIGHT  
OF URANIUM IN GRAMS

NORTH  
FACE

\*SERIES IV MONITORS  
WERE IRRADIATED  
OVER TWO ORR CYCLES  
(NOS. 24 AND 25)

Fig. 12A ORR Cycle 25; ORR Core Configuration.

		WEST FACE								
		1	2	3	4	5	6	7	8	9
SOUTH FACE	A				168.37	169.22	166.85			
	B			190.89	130.71	134.69	100.69	187.58		
	C			146.63	146.34	162.45	174.67	199.68	143.40	
	D		144.93	200.14	81.40	142.13	60.09	157.26	143.43	
	E		146.14	199.78	199.65	176.78	175.67	199.98	145.01	
	F								147.29	
	G									
		EAST FACE								
		SERIES IV*								

ORR CYCLE NO. 25  
(SECOND PART)

STARTUP DATE: 5-22-60  
SHUTDOWN DATE: 6-11-60

FIGURES SHOWN  
IN EACH POSITION  
REPRESENT THE WEIGHT  
OF URANIUM IN GRAMS

NORTH  
FACE

\*SERIES IV MONITORS  
WERE IRRADIATED  
OVER TWO ORR CYCLES  
(NOS. 24 AND 25)

Fig. 12B ORR Cycle 25; ORR Core Configuration.

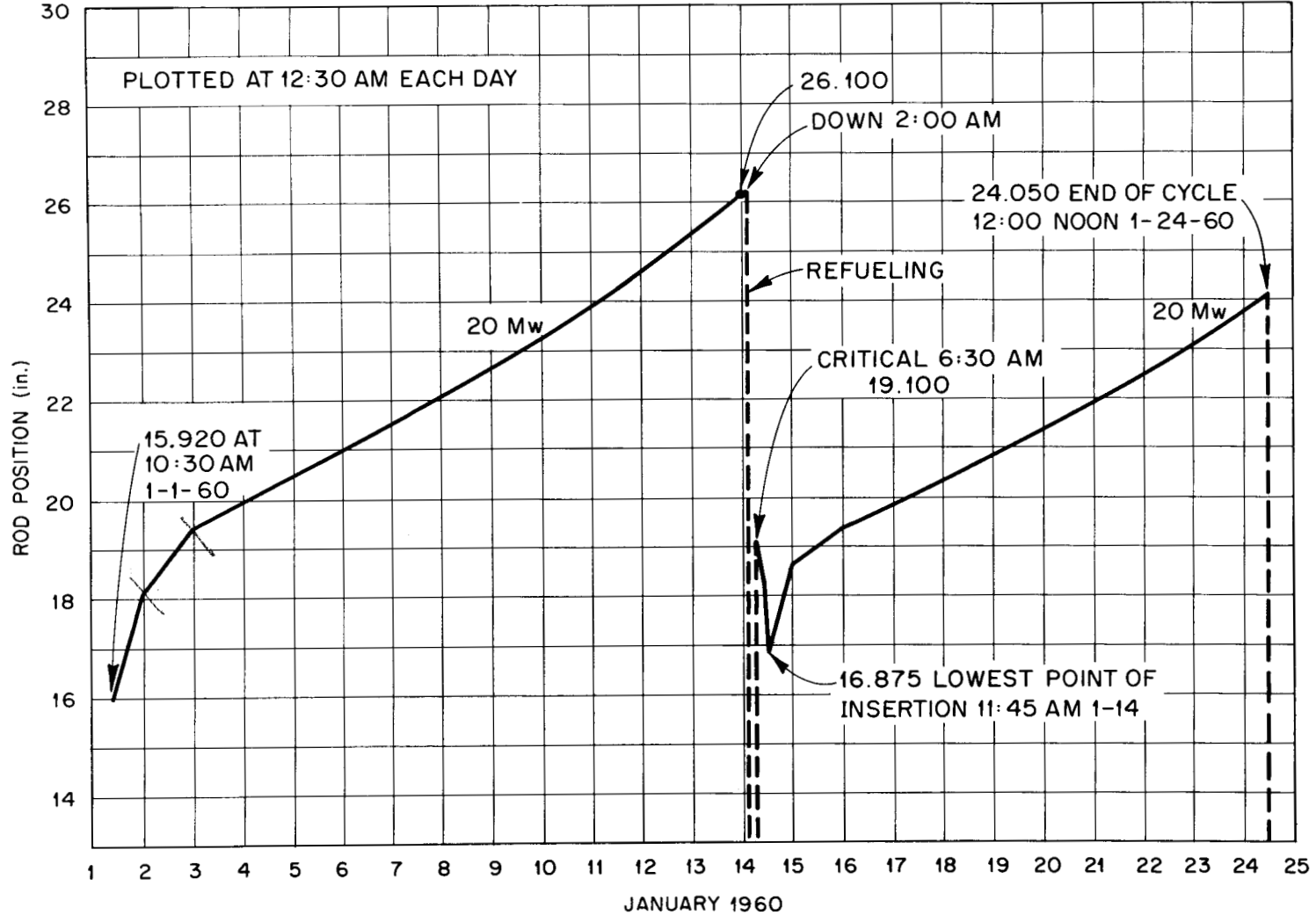


Fig. 13 Cycle XX; Rod Position vs Time (Series I).. REF: J. A. Cox,  
Reactor Operations and Radioactive Wastes Operations Quarterly Report  
January-March 1960, ORNL-CF-60-3-148 (May, 1960).

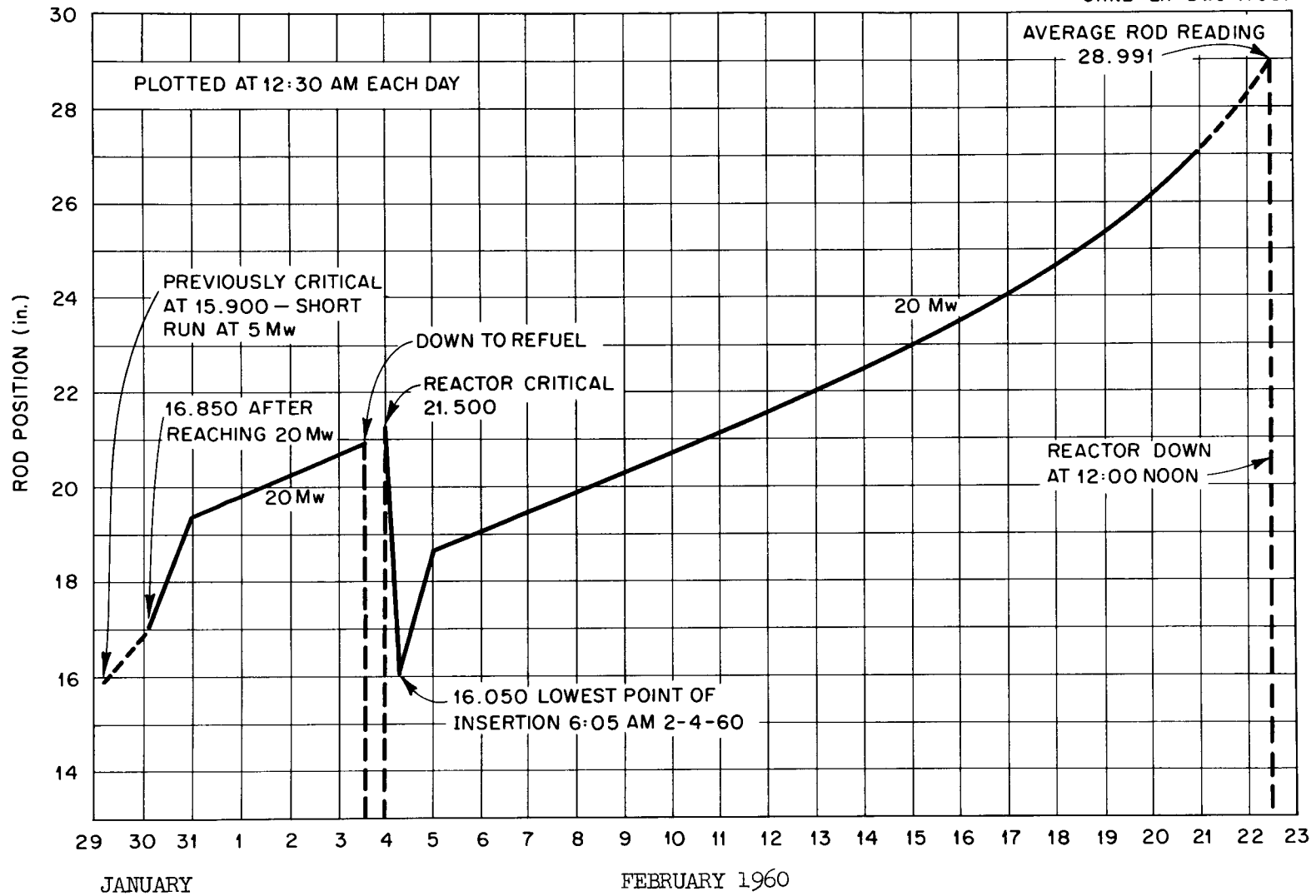


Fig. 14 Cycle XXI; Rod Position vs Time (Series II). REF: J. A. Cox, Reactor Operations and Radioactive Wastes Operations Quarterly Report January-March 1960, ORNL-CF-60-3-148 (May, 1960).

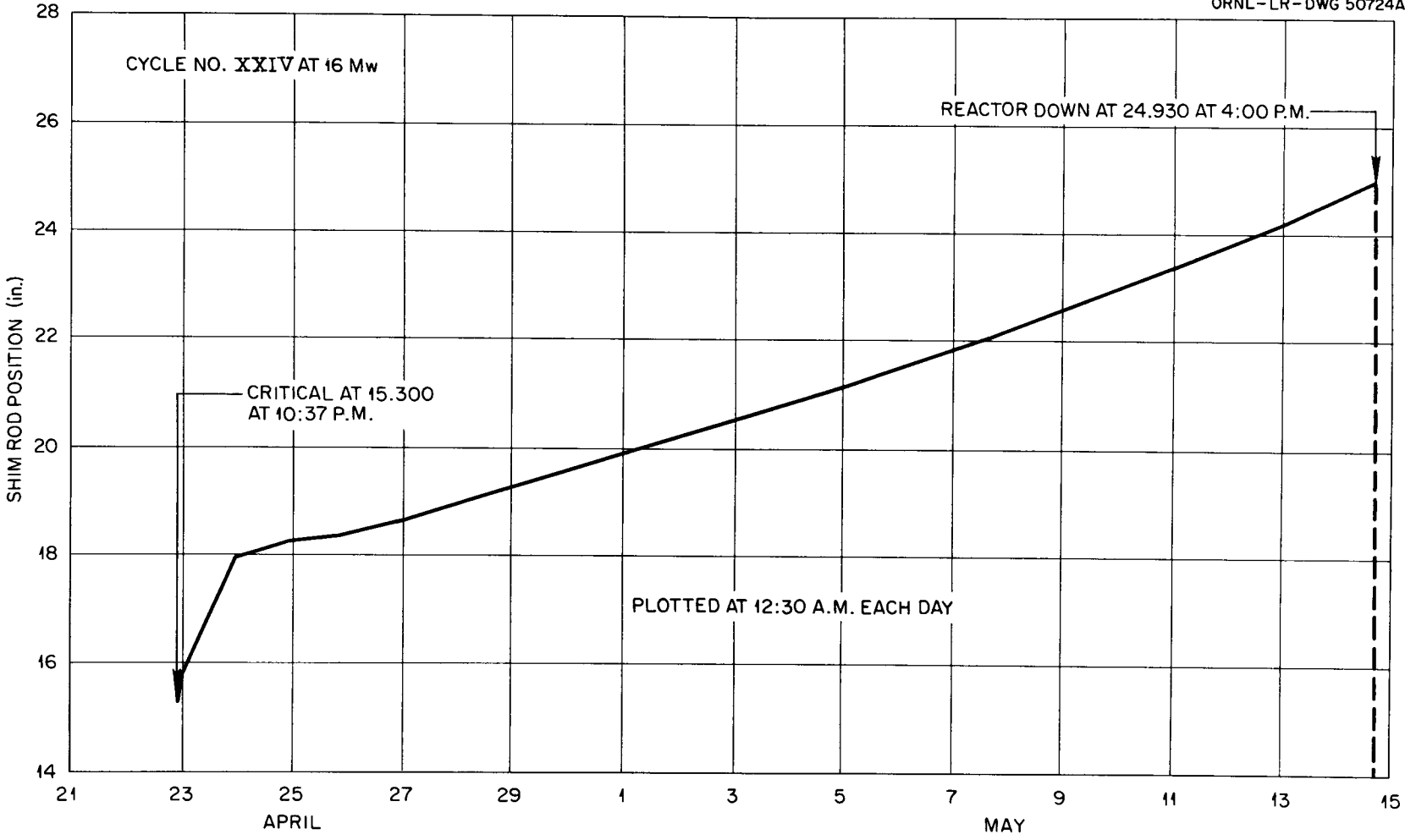


Fig. 15 Shim Rod Position vs Time (Series IV). REF: J. A. Cox, Reactor Operations and Radioactive Wastes Operations Quarterly Report April-June 1960, ORNL-CF-60-6-127 (August, 1960).

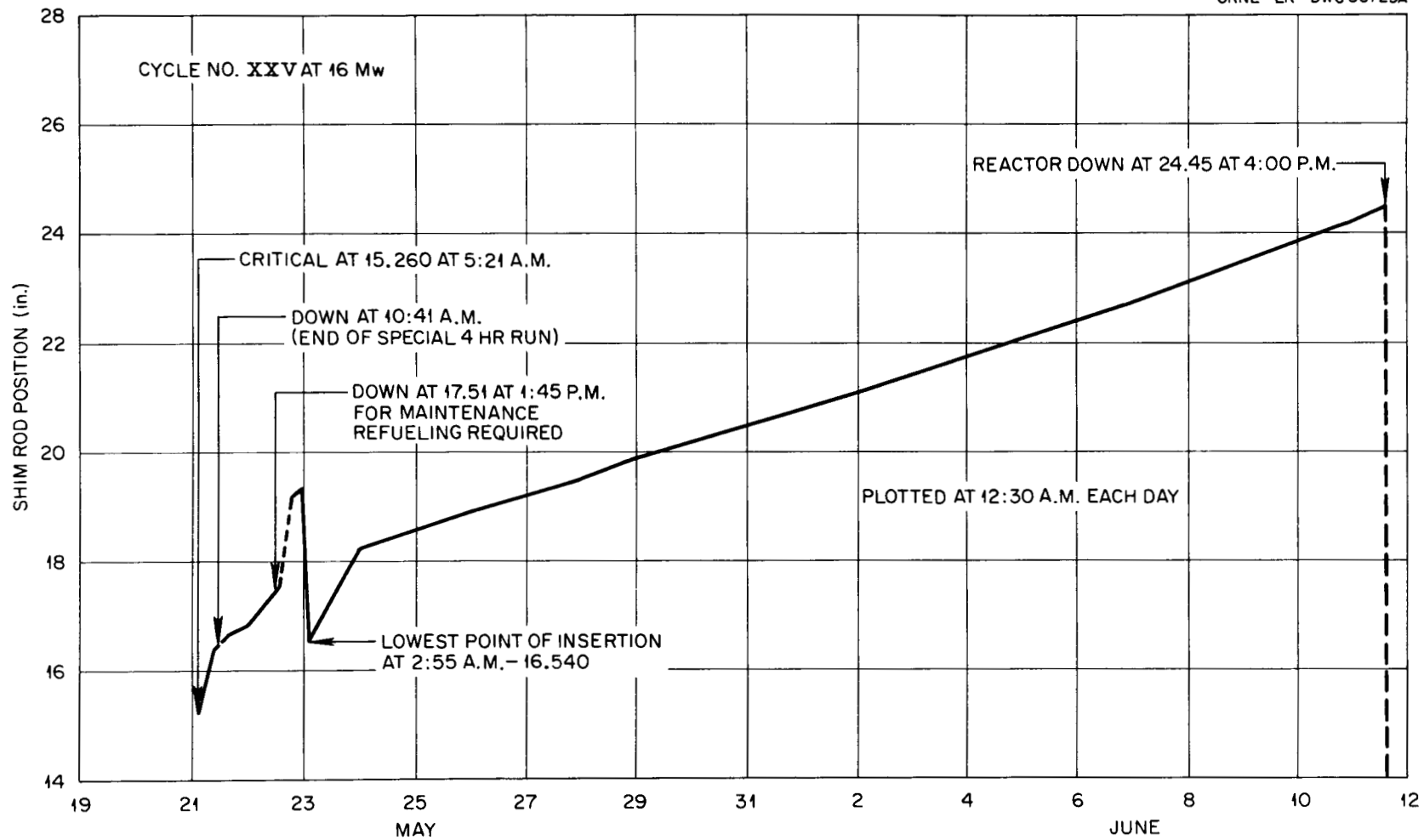


Fig. 15A Shim Rod Position vs Time (Series IV). REF: J. A. Cox, Reactor Operations and Radioactive Wastes Operations Quarterly Report April-June 1960, ORNL-CF-60-6-127 (August, 1960).

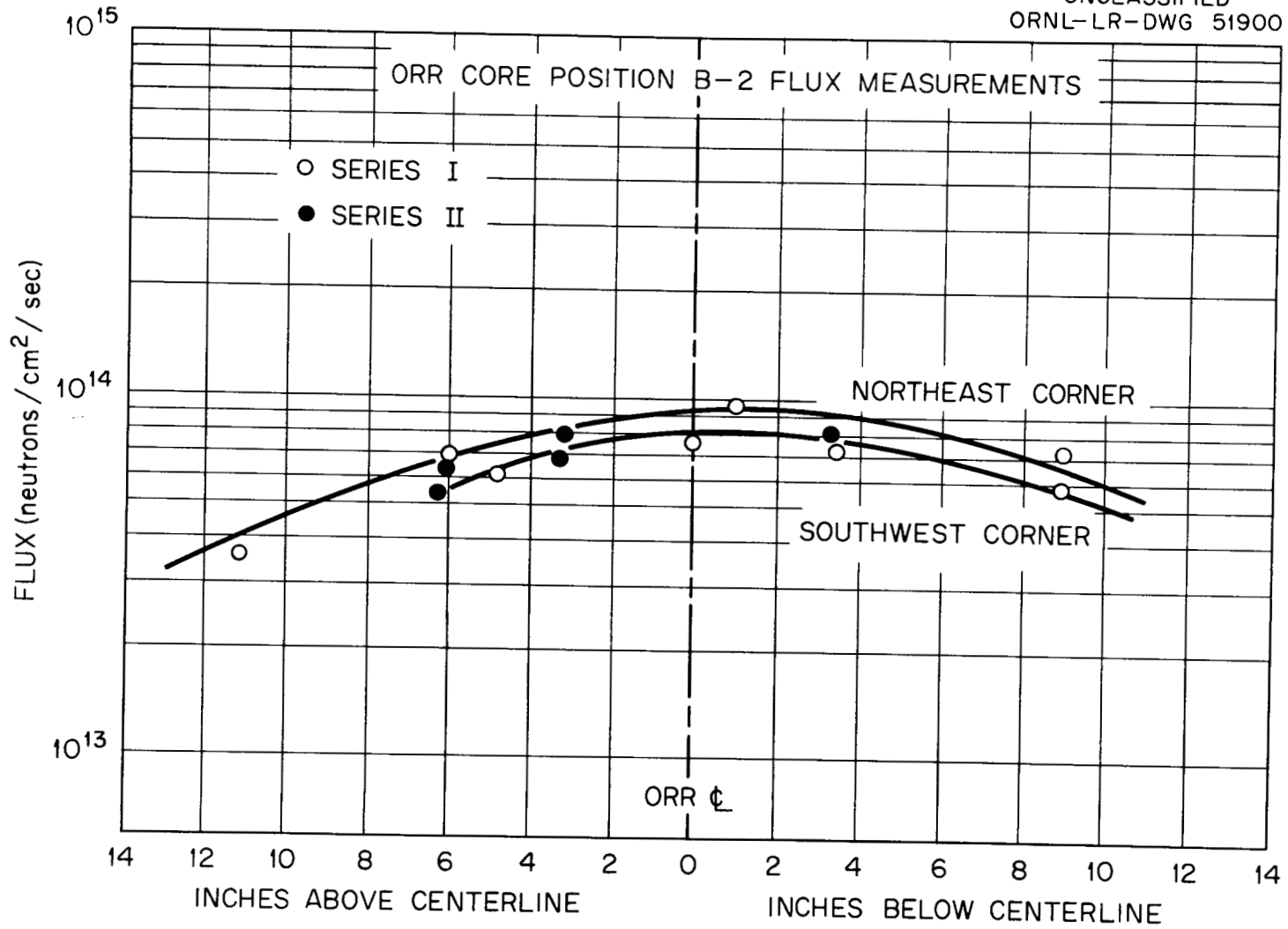


Fig. 16 Axial Thermal Flux Distribution as Measured with Cobalt - ORR Core Position B-2.

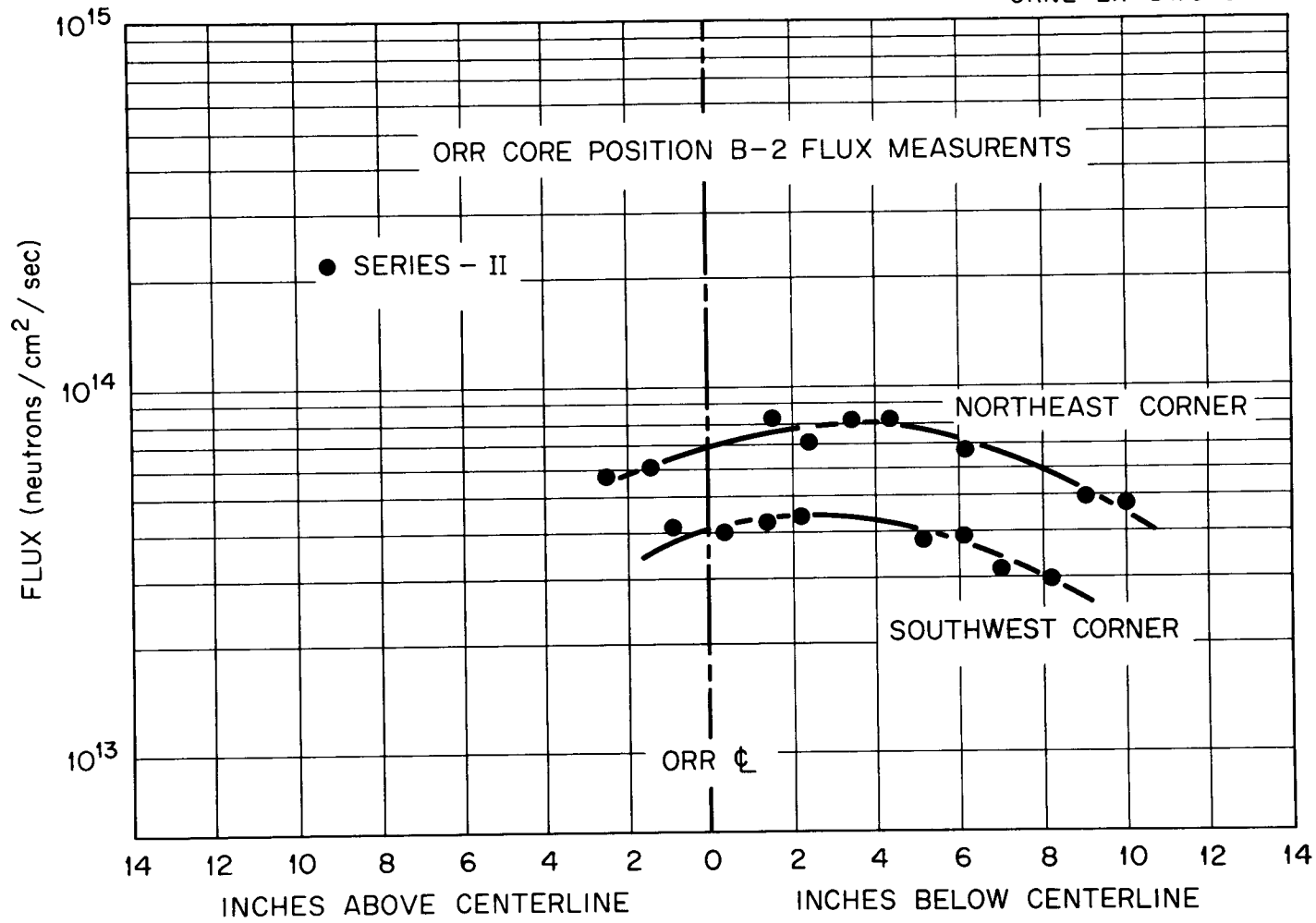


Fig. 17 Axial Flux Distribution (Energies Above 0.7 Mev) as Measured with Np<sup>237</sup> in B-2 Position.

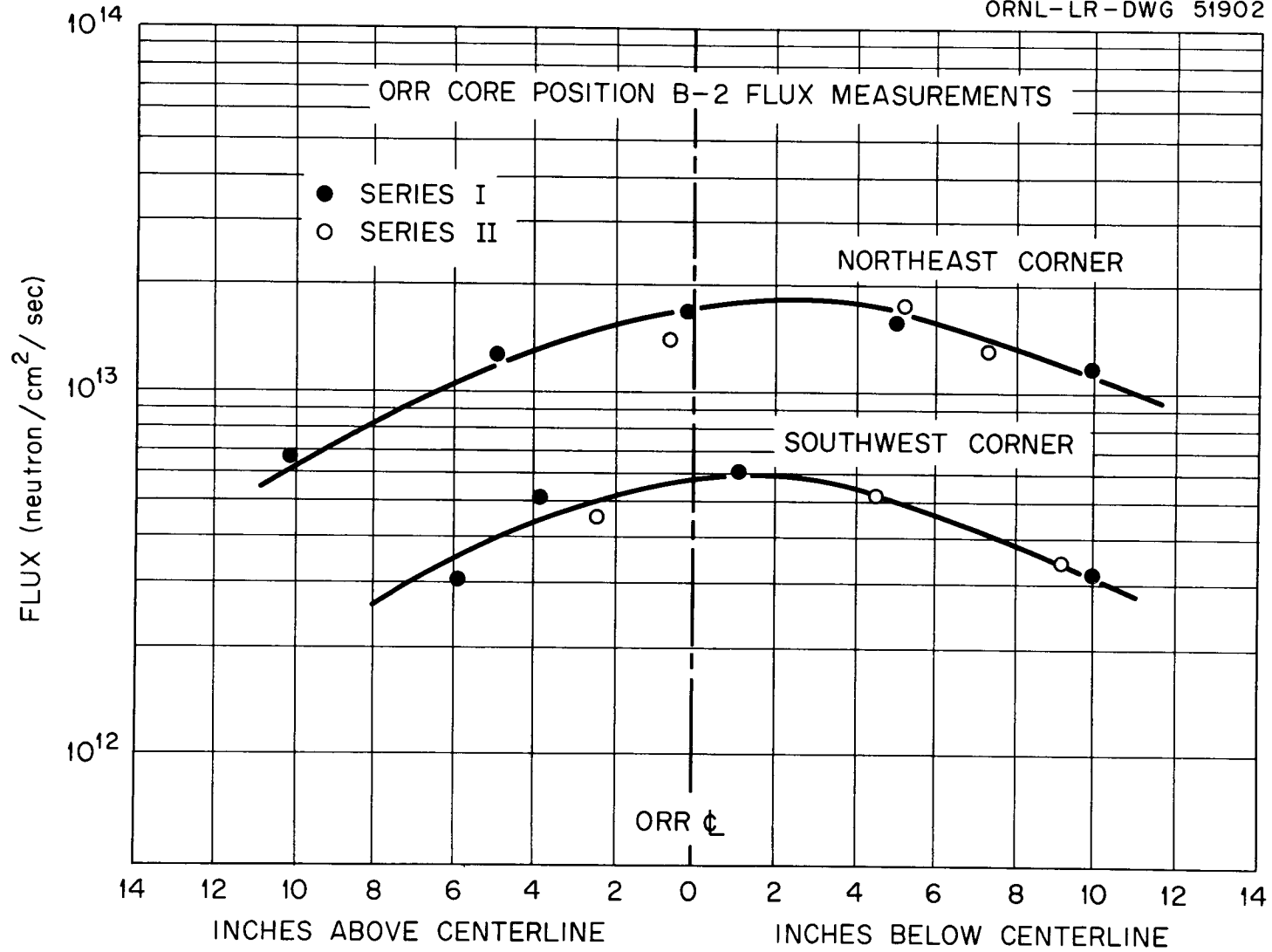


Fig. 18 Axial Fast Flux Distribution (Above 2.9 Mev) as Measured with  $S^{32}$  in B-2 Position.

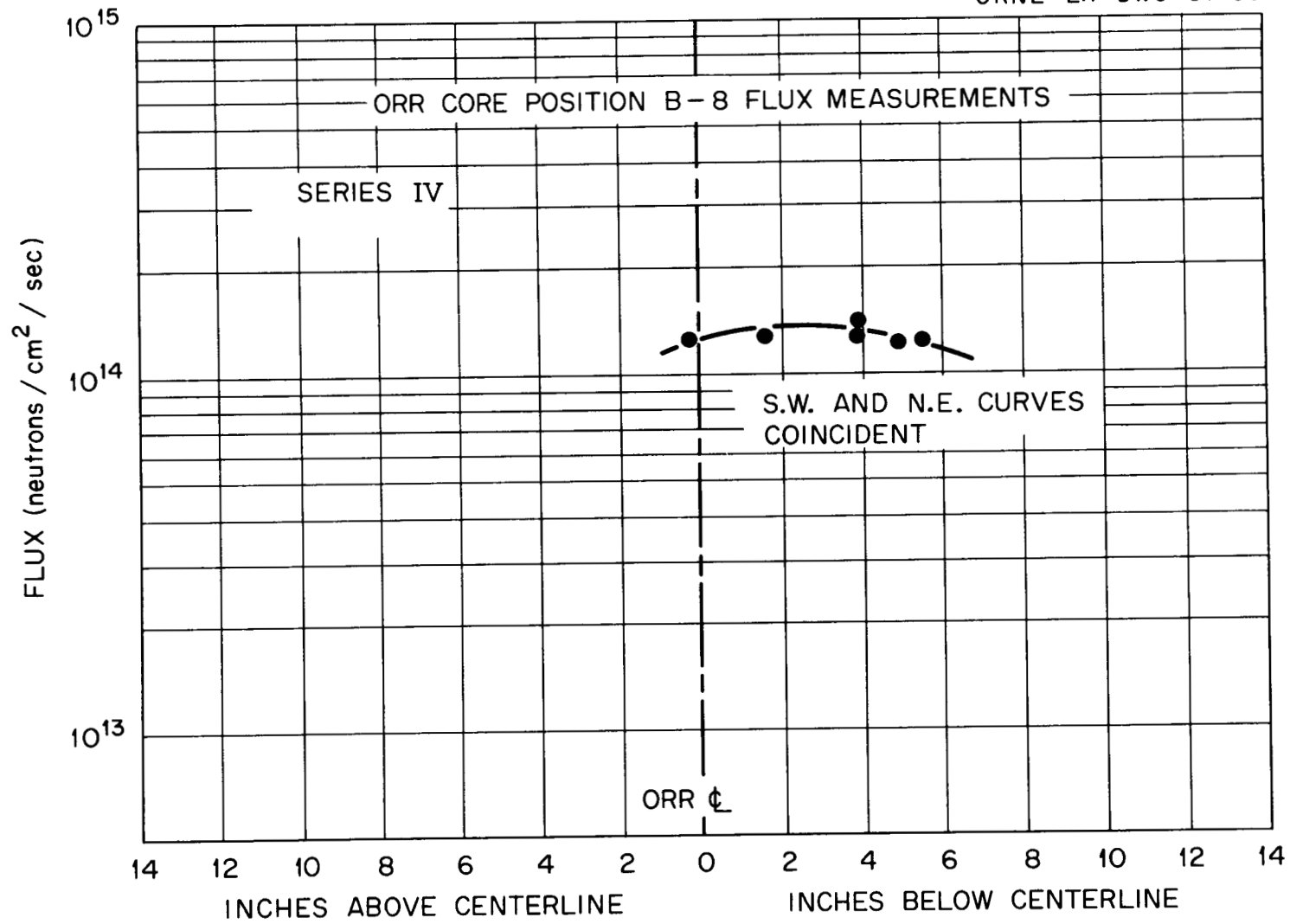


Fig. 19 Axial Flux Distribution (Energies Above 0.7 Mev) as Measured with Np<sup>237</sup> in B-8 Position.

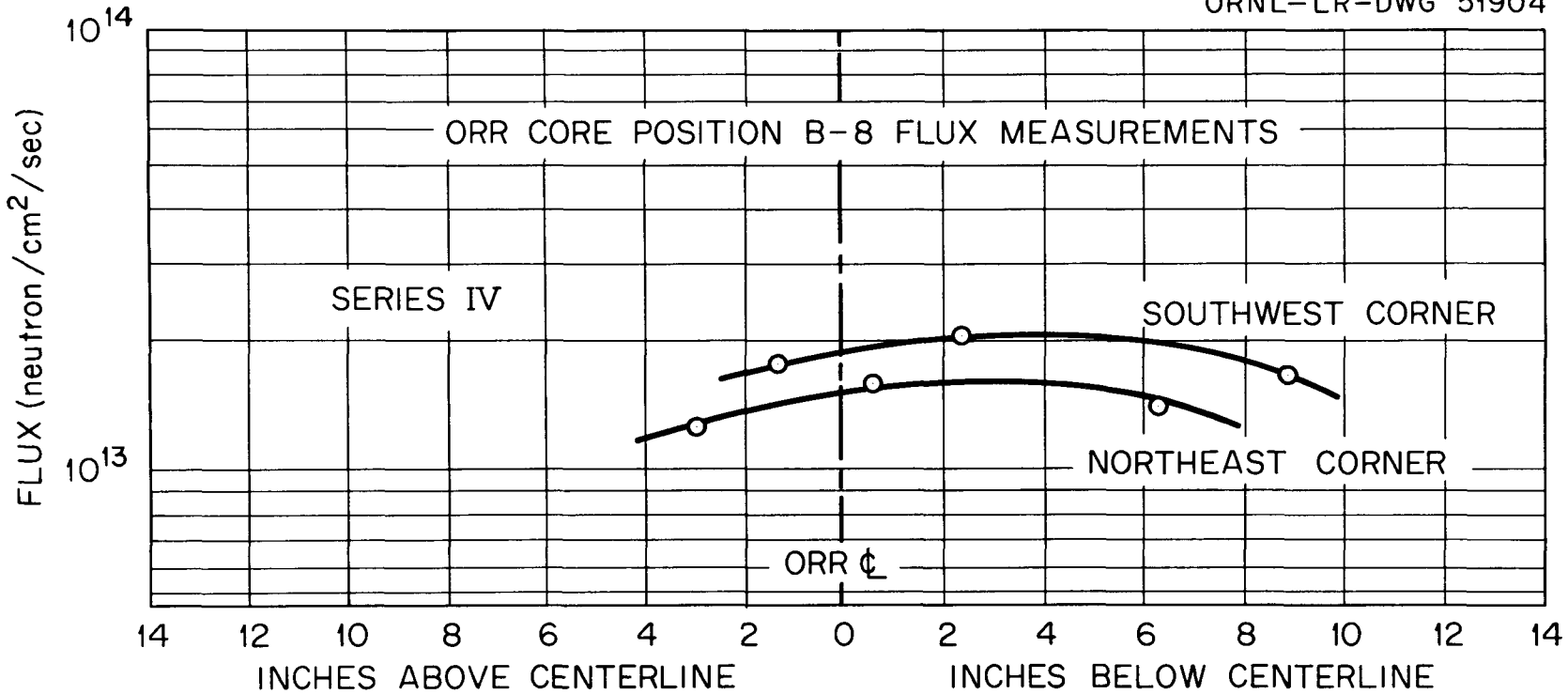


Fig. 20 Axial Fast Flux Distribution (Above 2.9 Mev) as Measured with  $S^{32}$  in the B-8 Position.

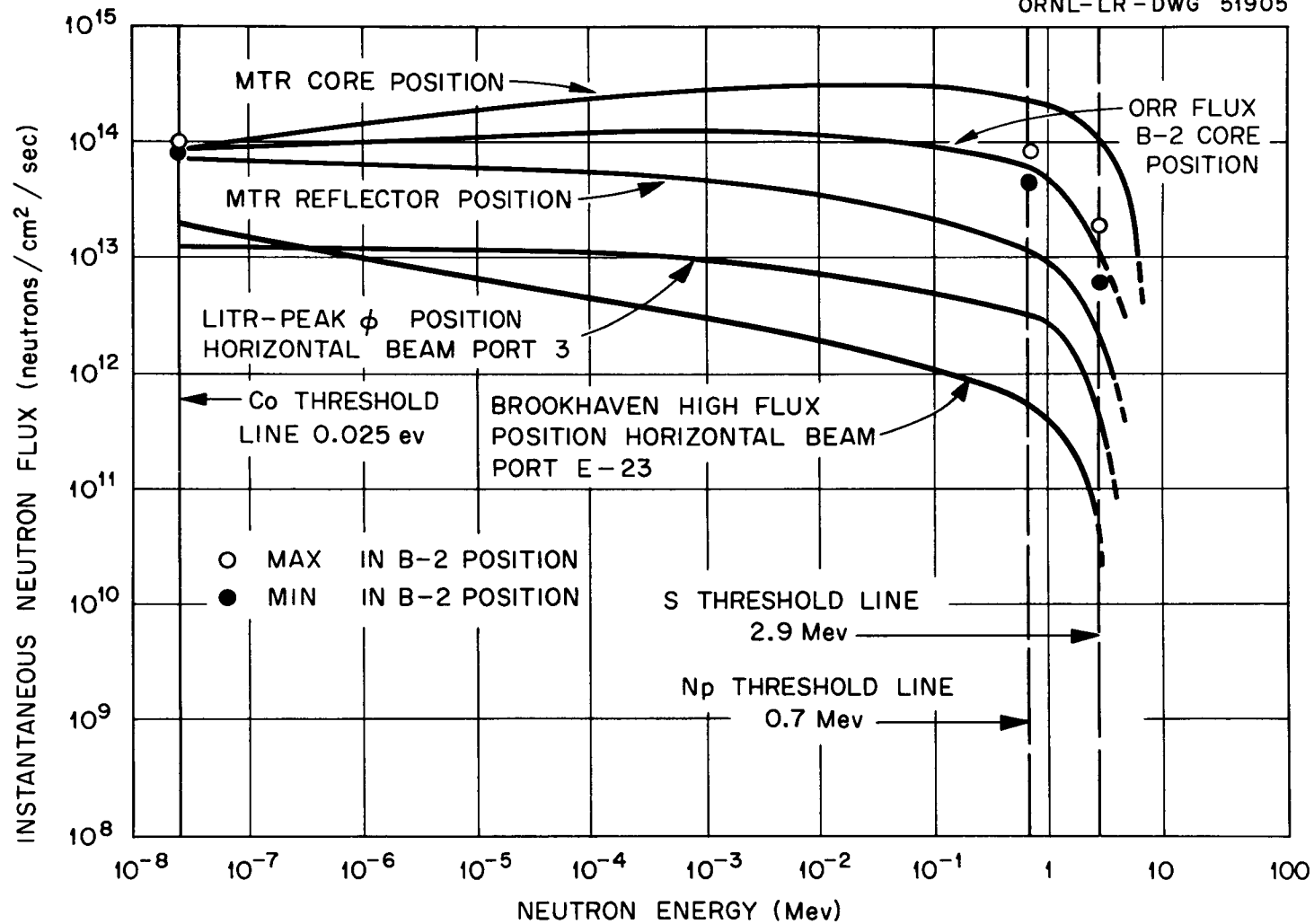


Fig. 21 B-2 Position Spectral Distribution Shown Compared with Data Obtained by L. E. Steele and J. R. Hawthorne. REF: L. E. Steele and J. R. Hawthorne, Neutron Flux Measurements for Materials Irradiation Experiments at ANL, BNL, ORNL, and NRTS, NRL-5483 (May, 1960).

and can be explained in terms of normal radial attenuation in flux magnitude, which is more pronounced in the higher energy flux groups. In the thermal region absorption is prevalent, while in the fast regions scattering to lower energy groups is more significant with respect to the observed attenuation. Other factors include experimental error and the effect of the reflector which is adjacent to the B-2 position.

Figures 19 and 20 represent the data obtained in B-8 and indicate generally greater flux magnitudes as predicted in the discussion presented earlier in this section. It was also noted previously that smaller gradients in flux should be observed between the northeast and southwest corners of the B-8 position than were measured in the B-2 position. Again, the results confirm this statement. The results in Fig. 20 (sulfur measurements) indicate a 25% spread while Fig. 19 shows superimposed curves or no attenuation. This can be explained by the fact that whatever differences exist between the northeast and southwest corners would be more defined in the higher energy flux curves because of the sharper radial gradient.

Determination of spectral distribution by threshold detectors is a questionable procedure especially when only a few data points are available. Experimental error and errors in interpolation can occur unless a large number of detectors are used. A full discussion of this problem has been published by Steele and Hawthorne of the Naval Research Laboratory.<sup>18</sup>

Figure 21 shows the spectral distribution in the B-2 position. Drawing of the shape was influenced by the surrounding distribution curves taken from the work of Steele and Hawthorne.<sup>18</sup> Although the distribution so drawn is crude, it is interesting to note that it lies midway between the MTR core position and reflector curves. The ORR is an MTR-type reactor and the B-2 position lies between the core and the reflector, indicating close agreement of results.

#### SUMMARY AND CONCLUSIONS

Sulfur and cobalt were chosen as monitoring materials because their physical and nuclear properties were compatible with the experimental objectives of the

<sup>18</sup>L. E. Steele and J. R. Hawthorne, Neutron Flux Measurements for Materials Irradiation Experiments at ANL, BNL, ORNL and NRTS, NRL-5483 (May, 1960).

beryllium studies, and because the equipment and technology for accurate analysis of these monitors were available. Neptunium and uranium-238 were added so that the spectral distribution could be drawn, thereby providing a way of checking the general magnitude of the flux as determined with the primary monitoring material, sulfur.

Of the four monitoring materials used only the  $U^{238}$  failed to produce satisfactory results and this failure has been attributed to the  $U^{235}$  content, which undergoes thermal fission, the products of which overshadow those produced by the fast-fission monitoring reaction.

The maximum flux in the B-2 position of the ORR core (at 20 Mw) is  $9.5 \times 10^{13}$  neutrons/cm<sup>2</sup>.sec at thermal energies as measured with  $Co^{59}$ ,  $8 \times 10^{13}$  neutrons/cm<sup>2</sup>.sec above 0.7 Mev as measured with  $Np^{237}$ , and  $1.8 \times 10^{13}$  neutrons/cm<sup>2</sup>.sec above 2.9 Mev as measured with  $S^{32}$ .

In the B-8 position, however, the flux measurements were made in the corners that did not receive the maximum flux. These measurements indicate  $1.4 \times 10^{14}$  neutrons/cm<sup>2</sup>.sec above 0.7 Mev as measured with  $Np^{237}$  and  $2 \times 10^{13}$  neutrons/cm<sup>2</sup>.sec above 2.9 Mev as measured with  $S^{32}$ . The B-8 spectrum has not been compared with that obtained in B-2 because measurements were not made in corresponding corners of the two positions and so would have little value.

The limited data obtained with four threshold monitors cannot yield a satisfactory spectral distribution, but information so obtained can be helpful when attempting to estimate flux levels in other positions or reactors. The results of these measurements illustrate the shift in spectral distribution which occurs not only between core positions but also radially across any single position. It is therefore very difficult to calculate fast-flux values for reactors, and more specifically, experimental positions, for which no data exist.

In most materials irradiation tests, the neutron flux is the principal experimental variable being studied and so it is evident that considerable attention should be given to the problem of measuring accurately, the fast flux to which the material is exposed.

#### ACKNOWLEDGMENT

The authors wish to acknowledge the work of D. G. Gates in handling the flux monitors and W. J. Hampton in processing the monitors.

INTERNAL DISTRIBUTION

1. C. E. Center
2. Biology Library
3. Health Physics Library
4. Metallurgy Library
- 5-7. Central Research Library
8. Reactor Experimental Engineering Library
9. ORNL Y-12 Technical Library Document  
Reference Section
- 10-29. Laboratory Records Department
30. Laboratory Records, ORNL R.C.
31. L. B. Emlet (K-25)
32. A. P. Huber (K-25)
33. J. P. Murray (Y-12)
34. G. M. Adamson, Jr.
35. S. E. Beall
36. R. J. Beaver
37. M. Bender
38. R. G. Berggren
39. J. O. Betterton, Jr.
40. D. S. Billington
41. D. Binder
42. A. L. Boch
43. E. G. Bohlmann
44. B. S. Borie
45. C. J. Borkowski
46. G. E. Boyd
47. R. B. Briggs
48. W. E. Brundage
- 49-53. J. J. Cademartori
- 54-58. C. E. Cagle
59. J. V. Cathcart
60. R. A. Charpie
61. G. W. Clark
62. R. E. Clausing
63. R. S. Cockreham
64. J. H. Coobs
65. R. A. Costner
66. F. L. Culler
67. J. E. Cunningham
68. W. W. Davis
69. J. H. DeVan
70. D. A. Douglas, Jr.
- 71-85. P. Dragounis
86. J. H. Frye, Jr.
87. R. J. Gray
88. W. R. Grimes
89. J. P. Hammond
90. W. O. Harms
- 91-95. M. R. Hill
96. N. E. Hinkle
97. E. E. Hoffman
98. A. Hollaender
99. A. S. Householder
100. H. Inouye
101. W. H. Jordan
102. C. P. Keim
103. M. T. Kelley
104. C. R. Kennedy
105. R. B. Korsmeyer
106. J. A. Lane
- 107-121. G. W. Leddicotte
122. S. C. Lind
123. R. S. Livingston
124. T. S. Lundy
125. H. G. MacPherson
126. W. D. Manly
127. R. W. McClung
128. R. V. McCord
129. D. L. McElroy
130. C. J. McHargue
131. A. J. Miller
132. E. C. Miller
133. R. L. Moore
134. K. Z. Morgan
135. M. L. Nelson
136. A. R. Olsen
137. P. Patriarca
138. D. Phillips
139. M. L. Picklesimer
140. P. M. Reyling
141. R. C. Robertson
142. A. W. Savolainen
143. J. L. Scott
144. H. E. Seagren

- |      |                  |          |                              |
|------|------------------|----------|------------------------------|
| 145. | E. D. Shipley    | 158.     | D. B. Trauger                |
| 146. | O. Sisman        | 159.     | A. M. Weinberg               |
| 147. | M. J. Skinner    | 160-174. | J. R. Weir, Jr.              |
| 148. | G. M. Slaughter  | 175.     | G. C. Williams               |
| 149. | C. O. Smith      | 176.     | R. O. Williams               |
| 150. | G. P. Smith, Jr. | 177.     | J. C. Wilson                 |
| 151. | A. H. Snell      | 178.     | C. E. Winters                |
| 152. | J. T. Stanley    | 179.     | J. W. Woods                  |
| 153. | J. A. Swartout   | 180.     | H. L. Yakel, Jr.             |
| 154. | A. Taboada       | 181.     | J. C. Zukas                  |
| 155. | W. H. Tabor      | 182.     | J. H. Koenig (consultant)    |
| 156. | E. H. Taylor     | 183.     | C. S. Smith (consultant)     |
| 157. | W. C. Thurber    | 184.     | R. Smoluchowski (consultant) |
|      |                  | 185.     | H. A. Wilhelm (consultant)   |

#### EXTERNAL DISTRIBUTION

- 186. D. F. Cope, Reactor Division, ORO
- 187. W. R. Doggett, North Carolina State College
- 188. J. F. Elliott, Massachusetts Institute of Technology
- 189. J. L. Gregg, Cornell University
- 190. M. Grotenhuis, Argonne National Laboratory
- 191. J. R. Hawthorne, Naval Research Laboratory
- 192. H. V. Lichtenberger, General Nuclear Engineering Corporation
- 193. W. A. Maxwell, General Nuclear Engineering Corporation
- 194. R. L. Murray, North Carolina State College
- 195. J. M. Simmons, DRD, AEC, Washington, D. C.
- 196. E. E. Stansbury, University of Tennessee
- 197. L. E. Steele, Naval Research Laboratory
- 198. D. K. Stevens, Metallurgy and Materials Branch Division of Research, AEC, Washington, D. C.
- 199-208. W. L. Webb, American Electric Power Service Corporation
- 209. Division of Research and Development, AEC, ORO
- 210-769. Given distribution as shown in TID-4500(15th ed.) under Metallurgy and Ceramics Category (75 copies OTS).